INFORMATION TO USERS

This manuscript has been reproduced from the microfilm master. UMI films the text directly from the original or copy submitted. Thus, some thesis and dissertation copies are in typewriter face, while others may be from any type of computer printer.

The quality of this reproduction is dependent upon the quality of the copy submitted. Broken or indistinct print, colored or poor quality illustrations and photographs, print bleedthrough, substandard margins, and improper alignment can adversely affect reproduction.

In the unlikely event that the author did not send UMI a complete manuscript and there are missing pages, these will be noted. Also, if unauthorized copyright material had to be removed, a note will indicate the deletion.

Oversize materials (e.g., maps, drawings, charts) are reproduced by sectioning the original, beginning at the upper left-hand corner and continuing from left to right in equal sections with small overlaps.

Photographs included in the original manuscript have been reproduced xerographically in this copy. Higher quality 6" x 9" black and white photographic prints are available for any photographs or illustrations appearing in this copy for an additional charge. Contact UMI directly to order.

Bell & Howell Information and Learning
300 North Zeeb Road, Ann Arbor, MI 48106-1346 USA
800-521-0600

MODIFICATIONS TO THE SIMPLE METHOD FOR BUOYANCY-DRIVEN FLOWS

By

Yi Qian SHENG, M. A. Sc.

A Thesis

Submitted to the School of Graduate Studies

in Partial Fulfilment of the Requirements

for the Degree

Doctor of Philosophy

McMaster University

DOCTOR OF PHILOSOPHY (1999) **(Mechanical Engineering)**	**McMaster University** **Hamilton, Ontario**
TITLE:	**Modifications To The SIMPLE Method For Buoyancy-Driven Flows**
AUTHOR:	**Yi Qian Sheng** **M. A. Sc. (University of Toronto)**
SUPERVISORS:	**Dr. G. Sheng** **Dr. M. Shoukri** **Dr. P. Wood**
NUMBER OF PAGES:	**Xi, 112**

ABSTRACT

Numerical analysis for turbulent buoyancy-driven flows shares many common topics with other computational fluid dynamics (CFD) fields. However, it has several special problems that must be dealt with. The major contribution of this thesis is the development of a new algorithm, SIMPLET, for buoyancy-driven flows.

The essence of the SIMPLE method lies in its coupling between the momentum and continuity equations. Almost all the algorithms of the SIMPLE family are based on one precondition, that is, the corrected velocity is obtained from the corrected pressure only. However, in buoyancy-driven flows, there are two major forces driving the fluid movement: the force caused by the temperature gradients and the force caused by the pressure (including kinetic pressure) gradients. In this thesis, the effect of the temperature correction on the velocity correction is considered during the derivation of the pressure linked equation. A modification to the SIMPLE algorithm -- SIMPLET -- was proposed.

The development of the SIMPLET is divided into two stages. The first version of SIMPLET was developed on the basis of the Boussinesq assumption. Since the temperature variation in the flow fields encountered in modern electronic equipment and other industrial facilities is large enough that the Boussinesq assumption is not

acceptable, the second version of SIMPLET was developed to remove this restriction so that it can be used for general cases. Because large temperature variations invariably cause turbulence, the flows with appreciable length scales are nearly always turbulent. As a preview of the application of the SIMPLET algorithm to real industrial problems, this thesis investigates several cases of turbulent mixed convection flows in a cavity problem using the RNG turbulence model. The test cases show that the SIMPLET method can speed up the energy equation convergence rate because of its linkage between temperature and velocity. When the convergence rate of the energy equation becomes the determinant in reaching a solution, the advantage of the SIMPLET method will be prominent.

ACKNOWLEDGEMENTS

I would like to express sincere thanks to the following individuals and organizations that have contributed to the completion of this study:

- Dr. G. Sheng, Dr. M. Shoukri and Dr. P. Wood for their supervision, guidance and financial assistance throughout the course of this research program.
- Dr. R. Judd, a member of the supervisory committee, for his supervision and guidance throughout the course of this research program.
- The Ontario Graduate Scholarship Program, The McMaster University Scholarship Program and the Department of Mechanical Engineering for their financial support.
- Dr. L. W. Shemilt, Dr. G. Round and Mr. P. Bewer for their understanding and support.
- The San Diego Supercomputer Center for offering the C90 computing facility.
- Fellow graduate students with whom I shared a pleasant study atmosphere.
- The staff of the Dept. of Mechanical Engineering, Dept. of Chemical Engineering and the Computer Science Department for their care and assistance.
- My wife, Yu Ying Hua, for her understanding, support and care.

TABLE OF CONTENTS

NOMENCLATURE

a	coefficient in discrete equation
A	cell area
b	constant in discrete equation
B	volumetric expansion coefficient
d	pressure coefficient in velocity correction expression
D	diffusion conductance
F	strength of the convection
g	gravitational acceleration
j	flux
Gr	Grashof number ($= g\beta \Delta T l^3 / \nu^2$)
k	turbulent kinetic energy
l	length
l_m	mixing length
L	length scale
p	pressure
P	Peclet number
Pr	Prandtl number

Ra Rayleigh number (= Gr Pr)

Re Reynolds number (= V l ρ/μ)

Ri Richardson number (= Gr / Re^2)

Res Residual

S source term

S_h source term in energy equation

S_C constant part of linearized source term

S_P coefficient of ϕ_P in linearized source term

t time

T temperature

u velocity component in x direction

U velocity vector

v velocity component in y direction

V viscous terms in momentum equation

w velocity component in z direction

x Cartesian Coordinate

y Cartesian Coordinate

z Cartesian Coordinate

Greek Symbols

α thermal diffusivity

Γ diffusion coefficient

δ	temperature coefficient in velocity correction expression
δ_{ij}	Kronecker delta
ΔT	temperature difference
ΔV	volume of control volume
ε	the dissipation rate of turbulent kinetic energy
ϕ	general dependent variable
μ	dynamic viscosity
ν	kinematic viscosity
ρ	density
σ_t	turbulent Prandtl number
τ	shear stress
τ_t	turbulent shear stress

Superscripts

'	variable correction
*	variable before correction

Subscripts

c	cold
e, w, n, s	control volume faces
E, W, P, N, S	grid points
eff	effective

f	fluid
h	hot
i	coordinate index
in	inlet
j	coordinate index
l	laminar
nb	neighbor grid points
r	reference
t	turbulent
w	wall

CHAPTER 1

INTRODUCTION

1.1 The CFD Method and its Applications

With the rapid development of computer hardware and Computational Fluid Dynamics (CFD) methods, more and more engineers and scientific researchers recognize numerical analysis as a cost-effective and convenient way of obtaining detailed information for describing complex fluid flows. Various commercial CFD software packages for different application fields are available nowadays such as FLUENT, PHOENIX, FLOWTHERM, FLOVENT, ANSYS etc..

Numerical heat transfer has emerged as a new field which has significant impact on scientific research and industrial product development. Thermal analyses have been traditionally applied to product design, such as turbine design, combustor design etc.. These products are operated under high temperature and forced convection is used to control the operating temperature. Because of rapid improvements to numerical heat transfer methodology in recent years, thermal analyses have become a modern technology to be applied for ordinary product design even when the products are operated at low temperature and natural convection or mixed convection are used for temperature control. One example of this is the rapid growth in electronic equipment design. Recent trends such as high power densities on the chip, the increasing use of multi-chip modules, surface-mount technology, avoidance of fans to reduce noise and reduced package

dimensions add to the thermal problem in electronic product development. Thermal analyses have played an important role in such product designs.

Buoyancy-driven flows are encountered in many engineering applications, such as building structures, space cooling and heating, nuclear reactors, radioactive waste containers, electronic equipment, solar collectors, the casting industry etc.. Estimates of the details of flow field are of crucial importance for evaluating equipment performance and designing products.

Buoyancy-driven flow is a particular kind of convective flow, where the buoyancy force cannot be neglected. The governing differential equations for convective flows involve the mass continuity equation, the momentum equations and the energy equation. The derivation of these equations is based on the conservation of mass, momentum, and energy respectively. The detailed derivation of these fundamental equations can be found in any fluid dynamics or heat transfer textbook (eg. [1]). If the flow is turbulent, turbulence model equations will also be involved. The solution of these equations under given boundary conditions (including initial conditions if the flow is unsteady) will provide detailed information about the distribution of pressure, temperature, velocity etc.. Based on this information, all the flow field behavior can be displayed with various computer software. Unfortunately, these governing equations can only be solved analytically, with significant simplifications, for a few cases [1,2]. The validity and reliability of this method of analysis depends on how well the differential equations and the boundary conditions represent the real physical phenomena. An oversimplified equation, a rough model, or an incorrect boundary condition assignment will lead to an inaccurate solution or even a wrong

conclusion. Oversimplification must be avoided and therefore, the governing equations with reasonable simplification are usually solved numerically. That means the solution procedure involves two steps: converting the differential equations to discrete algebraic equations and then solving the algebraic equations. Modern computer technologies and mathematical tools are now so powerful that the solution of these discrete algebraic equations is nearly always available if these equations are properly formulated. The solution we obtain in this way is usually called a numerical solution and, in fact, is the solution to the discrete algebraic equations and therefore an approximate solution to the original differential equations. If no round-off error is considered, the precision of the solution depends on how well the discrete algebraic equations represent the original differential equations.

The approach used to convert the differential equation to a discrete algebraic equation is called the discretization method. The most important discretization methods are the finite difference methods, including the finite volume method, and the finite element method. The finite element method was originally developed for computational solid mechanics use, but it has found more and more applications in the CFD field nowadays. The detailed description of these methods can be found in any CFD textbook (cf. [2],[3]). However, the most widely used method to solve buoyancy-driven flows and convective flows is still the finite volume method.

In the finite volume method, a computational domain is divided into a finite number of control volumes which are constructed by grid lines. The integral of each governing conservation equation is implemented for every control volume. The surface and volume

integrals are approximated using appropriate schemes and the differential equation is then converted to an algebraic equation. In the discrete equations, only the value of the variables at the grid nodes are involved. If we sum equations for all the control volumes, we obtain the global discrete algebraic equations for the whole computational domain. [3] The solution we are looking for is in fact the solution of the discrete equations and not the initial differential equations. Therefore, the validity and the reliability of this type of numerical solution depend not only on how well the differential equations and the boundary conditions represent the real physical phenomena but also how well the discrete algebraic equations represent the differential equations. All in all, the solution precision of a numerical method depends on how good the final equations we are solving are.

Once the discrete algebraic equations are created for a particular flow, the last problem is how to solve them. Though the solution scheme and procedure will not change the equations we are solving and therefore will not change and influence the solution precision, it is still an important part of the process. Without an efficient solution procedure, the equations may not be solved practically with limited computer facilities or may even not be solved at all. The current thesis concentrates on the topic of the solution scheme only.

1.2 Background to the Problem

The solution procedure for the governing equations is problem dependent. For turbulent, buoyancy-driven flows, the discrete algebraic equations are nonlinear and coupled. For such kinds of nonlinear and coupled algebraic equations, the most widely

used solution method is the sequential scheme [3] in which the equations are solved one by one with an iterative method. Each equation is linearized and solved for a single unknown only. All the other unknowns and even the unknown being treated, when used in a coefficient in the equation, are assigned the currently available values. After one iteration, all the coefficients are updated and all the equations are solved again. The iteration continues until all of the unknown variables are reasonably unchanged and no more iteration is needed. (i.e. the solution is said to be converged)

When the iteration method is used and the equations are solved one by one, the major problem is the lack of an independent pressure equation. In a laminar isothermal fluid flow problem for example, the four independent variables are the three components of the velocity vector plus the pressure while the four governing equations are comprised from the three momentum equations and the continuity equation. The mass continuity equation is only a constraint on the velocity field. An independent pressure equation may be developed by combining the momentum equations and the mass continuity equation as mentioned in [3]. The most widely used method is to develop and solve a pressure correction equation instead of an equation for the pressure itself [4].

In 1972, Patankar and Spalding [5] successfully developed the SIMPLE (Semi-Implicit Method for Pressure-Linked Equations) method using a staggered grid system. The essence of the method lies in its treatment of the coupling between the momentum and continuity equations. Since then, several variants of SIMPLE have been proposed to improve its convergence rate. In 1980, Patankar [4] introduced the SIMPLER method in which an extra equation was solved for the evaluation of pressure and the pressure-

correction equation is used for correcting the velocities only. In 1984, Van Doormaal and Raithby [6] proposed the SIMPLEC method to improve the consistency of the SIMPLE method. This modification usually provides faster convergence when the pressure-velocity coupling is the factor mainly responsible for slow convergence. In 1985, PISO, a method similar to SIMPLER, was proposed by Issa [7]. In the same year, Latimer and Pollard [8] developed a method called FIMOSE to introduce a new, fully implicit solution algorithm. In 1991, based on the minimization of the global residual norm , Chatvani and Turan [9] proposed a pressure-velocity coupling algorithm to determine the under relaxation factor in the pressure equation. In 1992, Lee and Tzong [10] introduced an artificial source term into the pressure-linked equation. In 1993, Yen and Liu [11] introduced an additional explicit correction step to decrease the number of iterations. It can be seen that all these modifications are based on one precondition: the velocity correction is evaluated with respect to the pressure correction only. There is no temperature-velocity coupling considered in the pressure-linked equation.

In parallel with the SIMPLE family of methods where the equations are solved one by one; simultaneous solution methods or partly simultaneous solution methods are also available [12-14]. In the CELS (Coupled Equation Line Solve) method developed by Galpin and Raithby in 1986[13], the temperature-velocity coupling was also considered. However, while they obtained good results for certain laminar natural convection cases, they made a statement in their paper [13] "……In natural convection flow, the momentum to energy coupling is strong for any significant convection. When the energy-to-momentum coupling is also strong, the T-v coupling is bidirectional and requires special

consideration for solution.....". In 1990, Davidson [14] applied the CELS method to turbulent flows, but the application was still for natural convection only. To the author's knowledge, there is no publication in the open literature about the application of CELS method to mixed convection flows where "the T-v coupling is bidirectional". Simultaneous solution methods were originally developed for solving linear coupled equations. When the equations are nonlinear and the iteration method must be combined into the simultaneous solution to linearize each of the individual equations, the method becomes difficult to use [3]. The technique of introducing under-relaxation factors to prevent divergence (as used in the sequential method) cannot be effectively applied to the simultaneous solution.

1.3 Major Contributions of This Work

In this thesis, an alternative method of coupling the temperature and velocity was developed. It still uses the sequential method. The central concept of this method is to modify the pressure linked equation in the SIMPLE algorithm to reflect the physical behaviour of two driving forces: the force caused by the pressure (including kinetic pressure) gradient and the force created by the temperature gradient in buoyancy-driven flows. The modified pressure linked equation considers the effects of both the pressure correction and the temperature correction on the velocity correction and therefore, this new method, called SIMPLET, is more appropriate for buoyancy-driven flows.

The major research efforts of this work have been summarized into two papers. One entitled "A Modification to the SIMPLE method For Buoyancy-Driven Flows" was

published in the Journal of Numerical Heat Transfer, Part B: Fundamentals, Vol. 33, PP 65-78, 1998. The other entitled "New Version of SIMPLET and Its Application to Turbulent Buoyancy-Driven Flows" was published in the Journal of Numerical Heat Transfer, Part A: Applications, Vol. 34, PP 821-846, 1998.

CHAPTER 2

SIMPLE ALGORITHM REVIEW

The development of the SIMPLET method is based on the SIMPLE algorithm. A short review of the SIMPLE method is given in this section to provide a context for SIMPLET. Most of the contents of this discussion are based on the textbook of Patanker [4] which should be consulted for the details.

2.1 The Discretization Equation

A detailed derivation of the governing differential equations can be found in [1]. In order to discuss the discretization of these equations, it is easier to mathematically write the equations in same form of [4] as follows:

$$\partial(\rho\phi)/\partial t + \text{div}\,(\rho U\phi) = \text{div}\,(\Gamma \text{grad}\,\phi) + S \qquad (1)$$

where ϕ is 1,u,v,T, k and ε respectively (if the k-ε turbulence model is used), Γ is the diffusivity which may be laminar or turbulent and S is the source term. The quantities Γ and S are specific to the particular meaning of ϕ but they will not influence the algorithm development.

For the purpose of illustration, two dimensional flow will be considered. Extension to three dimensions is straightforward. The governing differential equation for

a two-dimensional, steady flow in Cartesian coordinates can be simplified to:

$$\partial(\rho u\phi)/\partial x + \partial(\rho v\phi)/\partial y = \partial/\partial x(\Gamma\partial\phi/\partial x) + \partial/\partial y(\Gamma\partial\phi/\partial y) + S \qquad (2)$$

where ϕ, Γ and S can be summarized in the following table.

Table 1 Summary of the Governing Differential Equations

	ϕ	Γ	S	
Continuity Equation	1	0	0	
Momentum Equation in X Direction	u	μ_{eff}	$-\partial p/\partial x + \partial/\partial x(\mu_{eff}\,\partial u/\partial x) + \partial/\partial y(\mu_{eff}\,\partial v/\partial x) + \rho g_x$	
Momentum Equation in Y Direction	v	μ_{eff}	$-\partial p/\partial y + \partial/\partial x(\mu_{eff}\,\partial u/\partial y) + \partial/\partial y(\mu_{eff}\,\partial v/\partial y) + \rho g_y$	
Energy Equation	T	$\alpha\mu_{eff}$	0	cf eq. 61
Turbulence Kinetic Energy Equation	k	$\alpha_k\mu_{eff}$	$G_k + G_b - \rho\varepsilon$	cf. Eq. 49''
Turbulence Dissipation Rate Equation	ε	$\alpha_\varepsilon\,\mu_{eff}$	$C_{1\varepsilon}\varepsilon/k[G_k + (1- C_{3\varepsilon})G_b]- C_{2\varepsilon}^{*}\rho\varepsilon^2/k$	cf. Eq. 50''

According to the basic idea of the control volume method, the computation domain is divided into a number of cells as shown in Fig.1 and the differential equation is integrated over each cell which surrounds one grid point, (for example, P) to obtain the corresponding discretization equation.

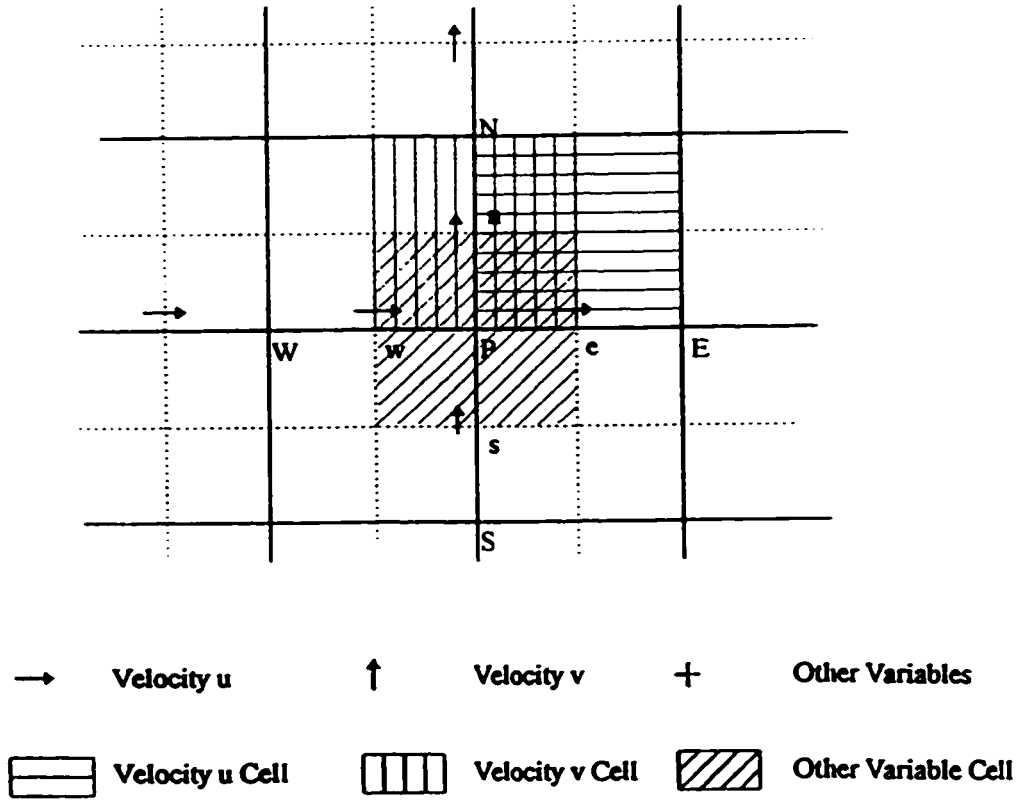

Fig. 1 Grid Distribution and Node Arrangement

The convection terms $\partial(\rho u\phi)/\partial x$, $\partial(\rho v\phi)/\partial y$ and the diffusion terms $\partial/\partial x(\Gamma\partial\phi/\partial x)$, $\partial/\partial y(\Gamma\partial\phi/\partial y)$ for each cell can be evaluated in terms of neighbor grid point values using a discretization scheme[4]. After linearizing the source term S as $S = S_C + S_P\phi_P$ and using the hybrid discretization scheme [4], we will have the following discrete equation:

$$a_P\phi_P = a_E\phi_E + a_W\phi_W + a_N\phi_N + a_S\phi_S + b \qquad (3)$$

or, in compact form as follows:

$$a_P\phi_P = \sum a_{nb}\phi_{nb} + b \qquad (3a)$$

where ϕ_P, ϕ_E, ϕ_W, ϕ_N and ϕ_S are the values of the variable ϕ at the grid point P and the four neighbor grid points, East, West, North and South respectively. The summation is over the appropriate neighbor points, nb, and the coefficients are given by

$$a_P = a_E + a_W + a_N + a_S - S_P\Delta V \qquad (4)$$

$$b = S_C\Delta V \qquad (5)$$

$$a_E = D_e\, A\,(|P_e|) + \langle -F_e, 0\rangle \qquad (6a)$$

$$a_W = D_w\, A\,(|P_w|) + \langle F_w, 0\rangle \qquad (6b)$$

$$a_N = D_n\, A\,(|P_n|) + \langle -F_n, 0\rangle \qquad (6c)$$

$$a_S = D_s\, A\,(|P_s|) + \langle F_s, 0\rangle \qquad (6d)$$

For the hybrid scheme (cf. [4]),

$$A\,(|P|) = \langle 0, 1 - 0.5|P|\rangle \qquad (7)$$

The special symbol $\langle\ \rangle$ stands for the largest of the quantities contained within it.

In equation (6), F is the mass flux at the grid face and D is the diffusivity coefficient given by

$$F = \rho u \tag{8}$$

$$D = \Gamma/\delta x \tag{9}$$

The ratio of F over D is defined as a Peclet number, P.

$$P = F/D \tag{10}$$

Different grid systems and discretization schemes will change the expression of each of the coefficients in the discrete equation but will not change the equation form (3) and affect the discussion of the solution procedure. Therefore, the introduction to the SIMPLE algorithm and the development of its modification as a means of solving the governing equations are based on the initial and popular ones in open literature. [4][6]

2.2 Pressure Linked Equation

Noting that each individual equation is nonlinear and the equation set is coupled, an iteration method is used to linearize each equation and solve the discrete algebraic equations sequentially until a converged solution is reached. The main problem with using this method is that there is no direct equation for the pressure, p, which is one of the dependent variables and its gradient forms a part of the source term in the momentum equations. The calculation of the velocity field depends on the unknown pressure field. The central part of the SIMPLE method is the development of a pressure linked equation to treat the coupling between the momentum and continuity equations.

The staggered grid system shown in Fig. 1 is used to develop the SIMPLE algorithm. The main grid points are arranged at the cross points of the main grid lines, while the velocity component grid points are shown by short arrows. The grids for

velocity components are arranged on grids that are different from the grids used for other variables. With respect to the main grid points, the u-velocity locations are staggered (displaced) in the x direction joining two adjacent main grid points. The velocity components v and w (if the computational domain is three dimensional) are similarly defined.

To develop the pressure linked equation, let ϕ be the velocity u and rewrite eq. (6a). After extracting the pressure term from b, the resulting discrete algebraic equation for the variable u and the control volume centered at e can be written as

$$a_e u_e = \sum a_{nb} u_{nb} + b + (p_P - p_E) A_e \qquad (11)$$

In eq. (11) the term $(p_P - p_E)A_e$ is the force acting on the control volume caused by the pressure gradient in the x direction, A_e being the area on which the force acts. It is obvious that due to the use of the staggered grid system, the expression of this term is concise and easy to compute. No interpolation for pressure is needed as p_P and p_E are nodal values.

Based on a guessed pressure p^*, this u-momentum equation can formally be solved to obtain a u^* that satisfies

$$a_e u_e^* = \sum a_{nb} u_{nb}^* + b + (p_P^* - p_E^*) A_e \qquad (12)$$

Now, introducing

$$p = p^* + p' \qquad (13)$$

where p' is a correction to the guessed pressure so that p is nearer to the correct value and defining

$$u = u^* + u' \qquad (14)$$

and subtracting eq.(12) from eq.(11), we obtain an equation for the velocity correction u_e':

$$a_e u_e' = \sum a_{nb} u_{nb}' + (p_P' - p_E')A_e \quad (15)$$

Assuming $\sum a_{nb} u_{nb}'$ is zero (cf. the SIMPLE method, Patanker [4]) gives

$$u_e' = A_e/a_e\,(p_P' - p_E') = d_e(p_P' - p_E') \quad (16)$$

where

$$d_e = A_e / a_e \quad (17)$$

Therefore,

$$u_e = u_e^* + d_e\,(p_P' - p_E') \quad (18a)$$

As discussed in ref. [4], the omission of $\sum a_{nb} u_{nb}'$ is acceptable, for it will not change the ultimate solution. (ie. in the converged solution all velocity corrections will be negligible) Similarly, for u_w ,v_n , and v_s we have

$$u_w = u_w^* + d_w(p_W' - p_P') \quad (18b)$$

$$v_n = v_n^* + d_n\,(p_P' - p_N') \quad (18c)$$

$$v_s = v_s^* + d_s\,(p_S' - p_P') \quad (18d)$$

To obtain an equation for the pressure correction, p', the corrected velocities given by eqs. (18) are substituted into the following discrete continuity equation:

$$(\rho u)_e A_e - (\rho u)_w A_w + (\rho v)_n A_n - (\rho v)_s A_s = 0 \quad (19)$$

It should be stated that this concise form of the discrete continuity equation is also the result of using the staggered grid system.

Finally after substitution of eqs. (18) into (19) we obtain the following pressure linked equation for the pressure correction

$$a_p p_P' = \sum a_{nb} p_{nb}' + b \tag{20}$$

where the coefficients are given by

$$a_p = \sum a_{nb} = a_E + a_W + a_N + a_S \tag{21}$$

$$a_E = (\rho A d)_e \tag{22a}$$

$$a_W = (\rho A d)_w \tag{22b}$$

$$a_N = (\rho A d)_n \tag{22c}$$

$$a_S = (\rho A d)_s \tag{22d}$$

and the source b is given by

$$b = c_W - c_E + c_S - c_N \quad \text{[-b also represents a mass source]} \tag{23}$$

where $c_E = (\rho u^* A)_e$ (24a)

$$c_W = (\rho u^* A)_w \tag{24b}$$

$$c_N = (\rho v^* A)_n \tag{24c}$$

$$c_S = (\rho v^* A)_s \tag{24d}$$

The solution of eq.(20) yields the pressure correction.

2.3 The Solution Procedure of the SIMPLE Method

The detailed solution procedure can be found in ref. [4]. Iterations start from guessed initial fields and the momentum equations are solved sequentially to obtain u^* and v^*. The pressure linked equation is then solved to obtain p'. Finally we make the corrections to the velocity field and pressure field using eqs.(13) and eq.(18) and then solve the energy equation and other equations (if any) to find the updated fields. Since the individual equations are nonlinear and the equation set is coupled, the coefficients in

the discrete equations (a_E, a_W,etc.) are related to the dependent variables and are based on the previous iteration and need to be updated. Sufficient iterations should be executed until a specified convergence criterion set is satisfied for all equations.

CHAPTER 3

THE SIMPLET ALGORITHM

In buoyancy-driven flows, there are two major forces which drive the fluid movement: the force created by the temperature gradient and the force caused by the pressure (including kinetic pressure) gradient. The central concept of the SIMPLET algorithm is to reflect this physical phenomenon in the pressure linked equation and the solution procedure.

3.1 The Modification of the Pressure Linked Equation

During the derivation of the pressure linked equation in the SIMPLE algorithm, only a pressure related term is extracted from the constant "source" term, b, (cf. Eq.(11)) in the discrete momentum equation and the remaining terms are considered constant during one iteration. This mathematical treatment adequately reflects the physical situation except for natural convection and mixed convection problems where the buoyancy driving force cannot be neglected and sometimes is the major force driving the flow. Noting that the velocity change is caused not only by a pressure change but also by a temperature change, the buoyancy driving force should also be extracted from the constant term, b, in addition to the pressure term. By introducing the Boussinesq approximation [15], the buoyancy force applied to the control volume centered at e is

$g_x \Delta V B(T_P+T_E)/2$ where g_x is the gravity component in the x direction, B is the derivative of density with respect to temperature at the reference temperature T_r (the volumetric expansion coefficient), T_P and T_E are the temperature at the grid point P and E. The reference temperature T_r is usually assigned T_∞ or some other well-defined temperature.

Introducing

$$T = T^* + T' \tag{25}$$

and defining

$$\beta_e = g_x B \Delta V/2 \tag{26}$$

eqs. (11-21) can then be rewritten as follows:

$$a_e u_e = \sum a_{nb} u_{nb} + b + (p_P - p_E) A_e + (T_P + T_E)\beta_e \tag{11'}$$

$$a_e u_e^* = \sum a_{nb} u_{nb}^* + b + (p_P^* - p_E^*) A_e + (T_P^* + T_E^*)\beta_e \tag{12'}$$

$$a_e u_e' = \sum a_{nb} u_{nb}' + (p_P' - p_E') A_e + (T_P' + T_E')\beta_e \tag{15'}$$

$$u_e' = d_e(p_P' - p_E') + \delta_e(T_P' + T_E') \tag{16'}$$

where

$$\delta_e = \beta_e / a_e \tag{17'}$$

so that u_e is determined from u_e^* and two corrections:

$$u_e = u_e^* + d_e (p_P' - p_E') + \delta_e (T_P' + T_E') \tag{18a'}$$

Similarly,

$$u_w = u_w^* + d_w (p_W' - p_P') + \delta_w (T_W' + T_P') \tag{18b'}$$

$$v_n = v_n^* + d_n (p_P' - p_N') + \delta_n (T_P' + T_N') \tag{18c'}$$

$$v_s = v_s^* + d_s (p_S' - p_P') + \delta_s (T_S' + T_P') \qquad (18d')$$

The final pressure linked equation keeps the same form as eq. (20)

$$a_p p_P' = \sum a_{nb} p_{nb}' + b \qquad (20')$$

where a_p , a_E , a_W , a_N , a_S are the same as in equations (21) and (22). However, b changes and is now given by:

$$\begin{aligned} b = \; & c_W - c_E + c_S - c_N \\ & + [(\alpha_W - \alpha_E + \alpha_S - \alpha_N)\ T_P' \\ & + \alpha_W T_W' - \alpha_E T_E' + \alpha_S T_S' - \alpha_N T_N'] \end{aligned} \qquad (23')$$

where c_E , c_W , c_N , c_S are the same as in eq. (24) and

$$\alpha_E = (\rho A \delta)_e \qquad (27a)$$

$$\alpha_W = (\rho A \delta)_w \qquad (27b)$$

$$\alpha_N = (\rho A \delta)_n \qquad (27c)$$

$$\alpha_S = (\rho A \delta)_s \qquad (27d)$$

It can be seen that the extra square bracketed term shown in eq. (23') is the only difference between the original pressure linked equation in SIMPLE and the new one for SIMPLET.

3.2 The Solution Procedure

In order to use the modified pressure linked equation, the solution procedure should also be modified. Referencing the detailed solution procedure of the SIMPLE method [4], the solution procedure of the SIMPLET method for two dimensional buoyancy flows can be summarized as follows:

1. Guess an initial field, including a pressure field p^* and a temperature field T^*.

2. Solve the momentum equation to obtain u^* and v^*.

3. Solve the energy equation to obtain T and evaluate $T' = T - T^*$.

4. Solve the pressure linked equation to obtain p'.

5. Correct the velocity field and the pressure field to obtain u, v, and p.

6. Solve the energy equation to obtain the temperature field T.

7. Solve other ϕ equations (if any, such as k, ϵ for turbulent flows).

8. Update properties to prepare for the next iteration.

Obviously, this procedure is very similar to the procedure of the original SIMPLE method. The major difference is that there is an extra step, step 3 to evaluate T'. It should also be noted that an approximation has been introduced in the evaluation of T'. We solve the energy equation at step 3 using u^* and v^* instead of u and v so that the u' and v' are omitted. When the solution approaches convergence, u' and v' approach zero. This kind of omission will not change the ultimate solution and is the spirit of the development of the original SIMPLE method [4].

The modified pressure linked equation should provide a more reasonable pressure correction in flows where buoyancy is important since it considers the effect of the temperature change on the velocity change. The corrected velocity field and pressure field are thus consistent. The energy equation is solved based on these consistent velocity and pressure fields and therefore the convergence rate of this equation should be improved. This will be shown for the laminar flow test cases in chapter 4 and the turbulent flow test cases in chapter 5.

CHAPTER 4

THE LAMINAR FLOW TEST CASES

The motivation of the SIMPLET algorithm development is to make the pressure linked equation adequate for buoyancy-driven flows and to provide a solver with a better numerical coupling of the temperature and velocity fields dominated by buoyancy. It is not to improve the precision of the solution. If we could solve the governing differential equations analytically, the solution would be an exact and precise one. Since we are using a discretization method to solve the equations numerically, the solution we obtain is the solution to the algebraic, discrete equations and therefore is an approximate solution to the original differential equations. The precision depends on how well the discrete equations represent the differential equations. The modification to the SIMPLE method introduced in this thesis does not modify the conversion of the original differential equations to the discrete algebraic equations in any way nor does it change the final discrete algebraic equations at all. Hence the precision will be neither influenced nor improved. In the test cases, there was no precision issue involved; the solution obtained with SIMPLE and SIMPLET yielded the same results. The purpose of the test cases is to show how the SIMPLET method is implemented and how good the convergence rate of the energy equation is when compared to SIMPLE.

The SIMPLET method for laminar buoyancy-driven flows was tested on two typical examples. The first involves a natural convection problem in a square cavity; while the second considers a mixed convection problem behind a vertical backward-facing step. The computer code was developed by the author in FORTRAN and the computations were carried out on the Cray C-90 supercomputer at the San Diego Supercomputer Center. The test cases did show that the solutions provided by SIMPLE and SIMPLET were the same, as expected.

4.1 Test Case I----The Heated Square Cavity Case

The heated square cavity problem is a typical two-dimensional, steady, buoyancy-driven flow. The left wall is maintained at a higher temperature T_h and the right wall is maintained at a lower temperature T_c. The top and bottom walls are insulated ($\partial T/\partial y = 0$). The fluid movement inside the cavity is caused by the temperature difference between the right wall and the left wall. The problem was solved for air with $P_r = 0.71$ using an array of 32 X 32 irregularly spaced grids. The non-uniformity of the grids is generated in an exponential fashion with the refined grids near the wall boundaries. By introducing the Boussinesq approximation, the governing equations for a steady two-dimensional flow can be written as follows:

$$\partial u/\partial x + \partial v/\partial y = 0 \tag{28}$$

$$\partial(uu)/\partial x + \partial(uv)/\partial y = -1/\rho\,\partial p/\partial x + \mu/\rho(\,\partial/\partial x(\partial u/\partial x) + \partial/\partial y(\partial u/\partial y)) \tag{29}$$

$$\partial(uv)/\partial x + \partial(vv)/\partial y = -1/\rho\,\partial p/\partial y + \mu/\rho\,(\partial/\partial x(\partial v/\partial x) + \partial/\partial y(\partial v/\partial y)) + gB(T - T_r)/\rho \tag{30}$$

$$\partial(uT)/\partial x + \partial(vT)/\partial y = \alpha(\partial/\partial x(\partial T/\partial x) + \partial/\partial y(\partial T/\partial y)) \quad (31)$$

The boundary conditions are given by

$$x = 0; \qquad u = 0, \; v = 0, \; T = T_h \quad (32)$$

$$x = l; \qquad u = 0, \; v = 0, \; T = T_c \quad (33)$$

$$y = 0; \qquad u = 0, \; v = 0, \; \partial T/\partial y = 0 \quad (34)$$

$$y = h = l; \qquad u = 0, \; v = 0, \; \partial T/\partial y = 0 \quad (35)$$

The convergence is usually judged by the residual, Res, or the normalized residual, Res_{norm}. The residual, Res, is the imbalance in the discrete equation eq.(3), $Res = |a_E\phi_E + a_W\phi_W + a_N\phi_N + a_S\phi_S + b - a_P\phi_P|$, and the normalized residual, Res_{norm} is determined by $Res_{norm} = Res / |a_P\phi_P|$. For the pressure correction equation, the residual, Res, is the imbalance in the discrete continuity equation eq.(19), $Res = |(\rho u)_e A_e - (\rho u)_w A_w + (\rho v)_n A_n - (\rho v)_s A_s|$, and the normalized residual, Res_{norm} is determined as follows since there is no $a_P\phi_P$ available.

$Res_{norm} = Res/ (Res)_2$

where $(Res)_2$ is the residual at the second iteration.

Both Res and Res_{norm} should be summed over all of the computational grid points.

The convergence criteria used in this thesis were taken from the default ones set in the FLUENT software package [16] as they represent industry standards:

$Res_{norm} = 1.0 \cdot 10^{-3}$ for u, v, p

$Res_{norm} = 1.0 \cdot 10^{-6}$ for T

The test was first performed for the case of Rayleigh number, Ra, equal to $1.0 \cdot 10^6$, where

$Ra = G_r Pr$

$G_r = g\beta\Delta T\, l^3/\nu^2$	the Grashof number
$Pr = C_p\, \mu\, /k$	the Prandtl number
$\beta = -(\partial\rho/\partial T)_p/\rho$	the thermal expansion coefficient
C_p	specific heat at constant pressure
k	thermal conductivity
μ	dynamic viscosity
ν	kinematic viscosity

The problem was also solved with the commercial CFD package FLUENT choosing the options of SIMPLE and SIMPLEC to obtain solutions for comparison. No Boussinesq approximation is introduced in the FLUENT solution procedure. The residual histories for the two options, SIMPLE and SIMPLEC, using FLUENT are shown in Fig. 2(a). It can be seen that the application of these two methods resulted in almost the same convergence rates, particularly for the temperature, T.

Using the same grid distribution and the same discretization scheme but introducing the Boussinesq approximation, a computer code was written to solve the same problem using the SIMPLE and SIMPLET algorithms. The residual histories for these cases are plotted in Fig.2(b). A noticeable increase in the convergence rate was obtained when using the SIMPLET method. Further tests for different Rayleigh numbers were then executed and the residual histories for these cases are shown in Figs. 3-5. The required iterations for different Rayleigh numbers are summarized in the Table 2. Note that in each case significantly fewer iterations were needed when the SIMPLET method

was used. In every case, the underrelaxation factors for the two methods, SIMPLE and SIMPLET, were kept the same since the convergence rates are related to the underrelaxation factors being used. The results show that for the same SIMPLE method, the introduction of the Boussinesq approximation improves the convergence rate, especially in the initial stages of the iteration. For all the cases shown in Fig.3-5, the SIMPLET method provides faster convergence rate compared to the conventional SIMPLE method. Fig.6 and Fig.7 show the contour plots of temperature for Rayleigh number, Ra, equal to $1.0 \cdot 10^4$ and $1.0 \cdot 10^6$ respectively. Both SIMPLE and SIMPLET provided the same plots. Comparing to the corresponding bench mark plots shown in the ref. [17], there are only slight differences between our calculations and the bench mark solutions since the viscosity was considered as a constant in the ref. [17] and allowed to vary with temperature in our calculations. As expected, steep temperature gradients exist in the near wall region. These get even steeper as the Rayleigh number increases.

Table 2 Required Iterations for Test Case I

Ra	$1.0 \cdot 10^4$	$1.0 \cdot 10^5$	$1.0 \cdot 10^6$	$1.0 \cdot 10^7$
SIMPLE	420	375	380	340
SIMPLET	215	170	200	245

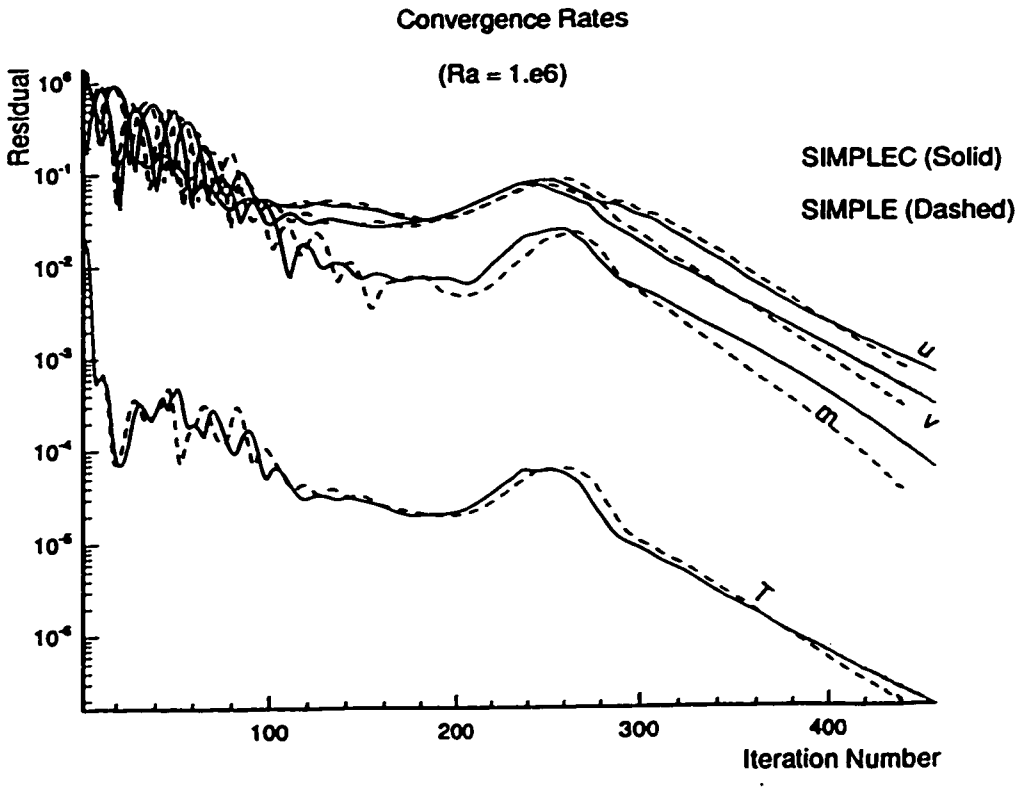

Fig. 2 Residual Histories for Test Case I (Ra = $1.0 \cdot 10^6$)

(a) Solved with SIMPLE and SIMPLEC (Using FLUENT)

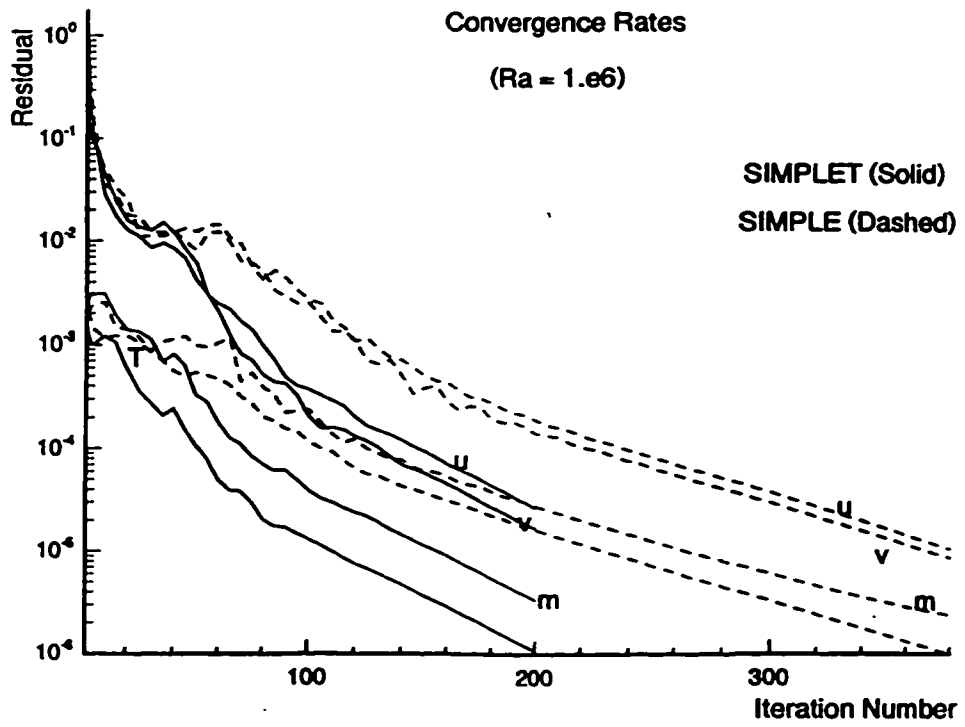

Fig. 2 Residual Histories for Test Case I (Ra = $1.0 \cdot 10^6$)

(b) Solved with SIMPLE and SIMPLET

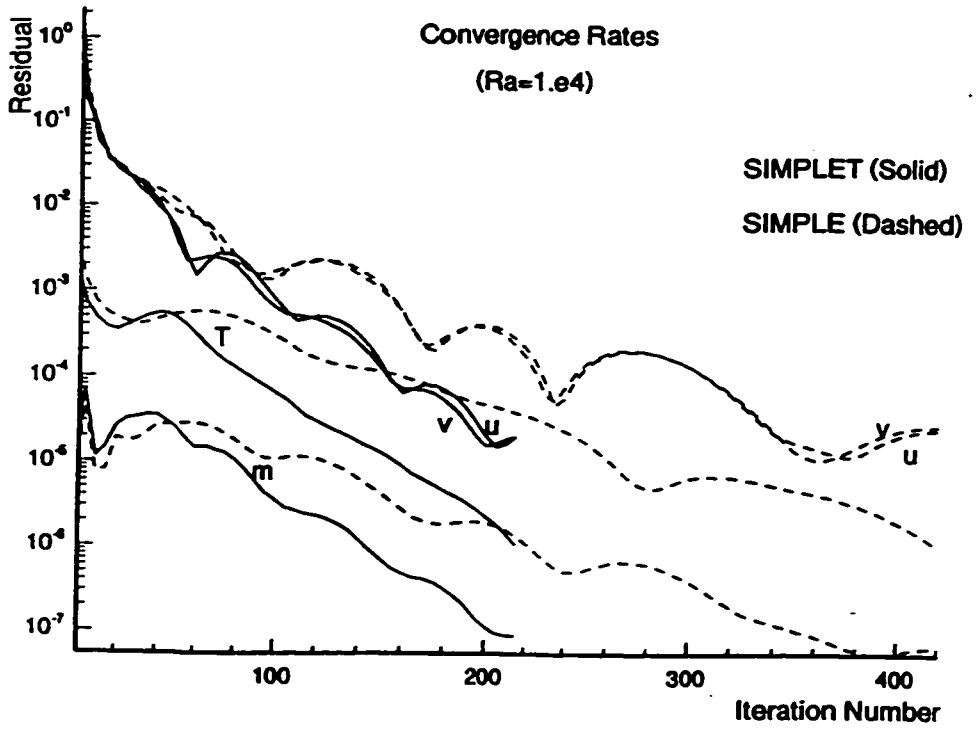

Fig. 3 Residual Histories for Test Case I (Ra = $1.0 \cdot 10^4$)

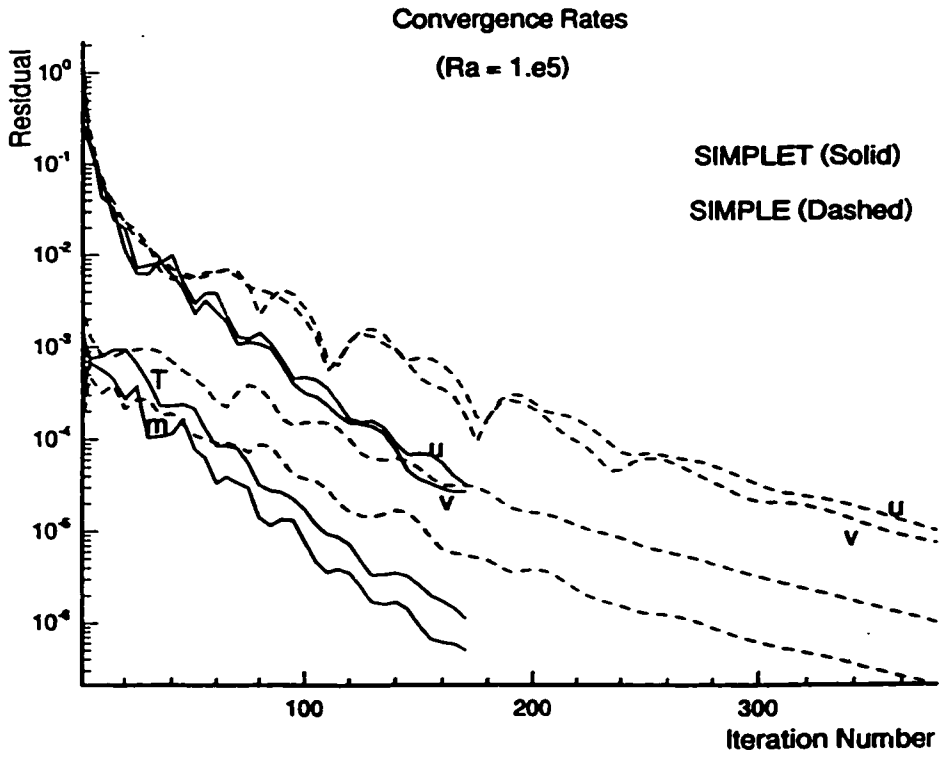

Fig. 4 Residual Histories for Test Case I (Ra = $1.0 \cdot 10^{5}$)

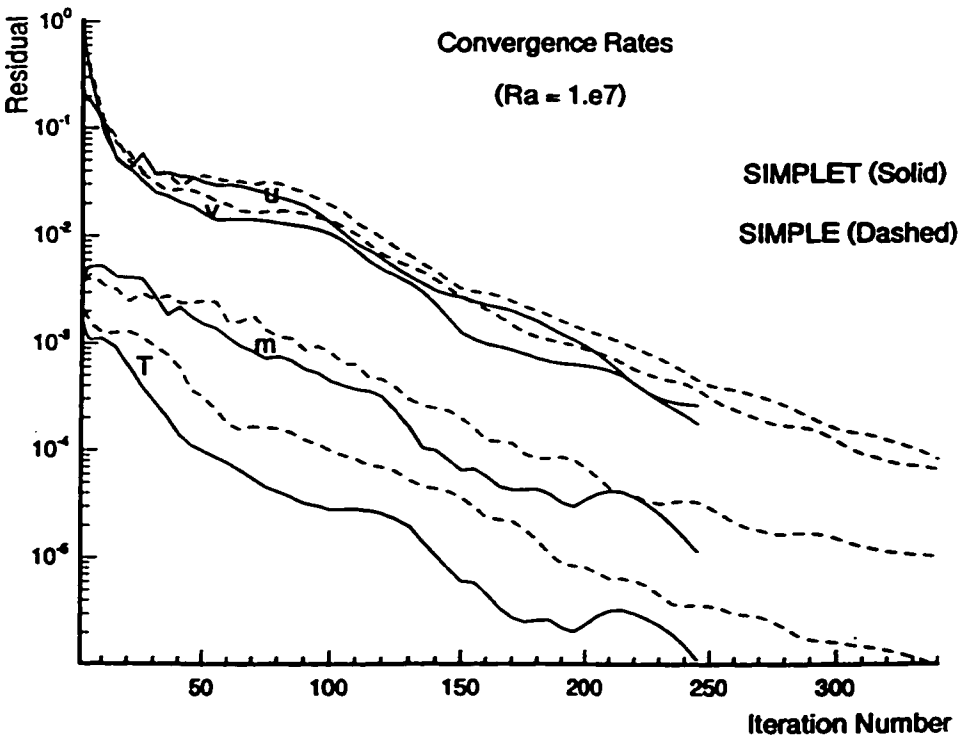

Fig. 5 Residual Histories for Test Case I (Ra = $1.0 \cdot 10^{7}$)

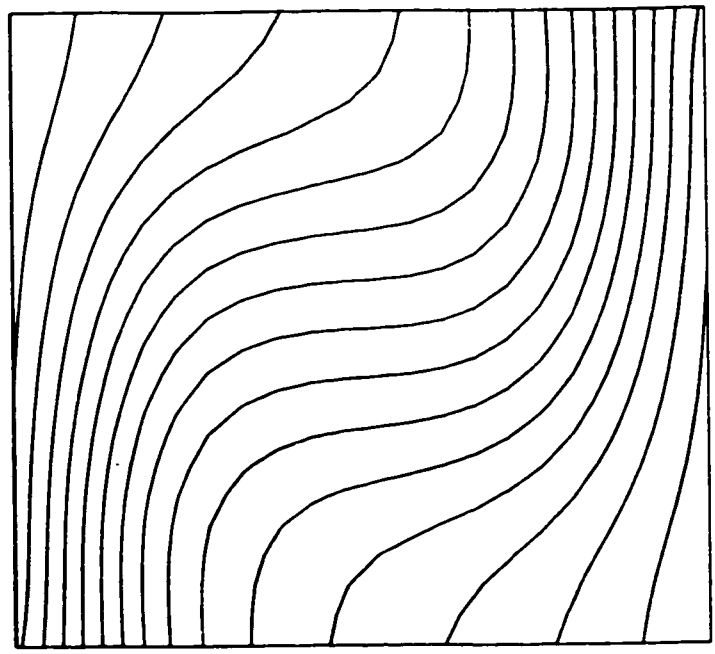

Fig. 6 Contour Plot of Temperature for Test Case I (Ra = 1.0 e4)

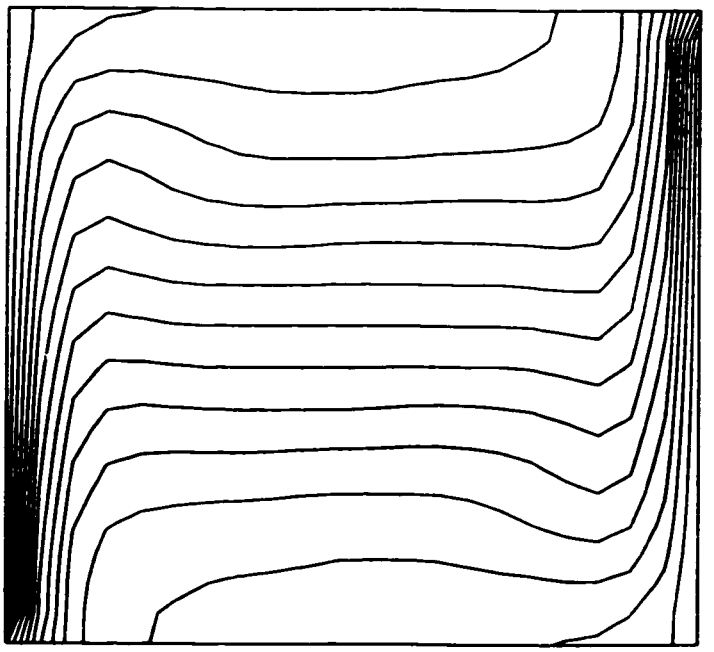

Fig. 7 Contour Plot of Temperature for Test Case I (Ra = $1.0 \cdot 10^6$)

4.2 Test Case II----The Mixed Convection Case Behind A Vertical Backward-Facing step

Test case II, a mixed convection problem behind the vertical, backward-facing step , is shown in Fig. 8. It was originally chosen from Ref. [18] . In the paper, the local axial conduction along the wall DF was not provided but was used in the computation (PP. 44). Because of this unavailable information, the boundary condition for the hot wall was changed from fixed heat flux in the original paper to fixed temperature in the test case II. This change also meets the requirement of the SIMPLET algorithm development to investigate the application of SIMPLET to the mixed convection flows with different Richardson numbers. The test cases were solved for air using a 72 X 29 grid array with the refined grids around the walls.

The governing equations for this two-dimensional, steady, mixed convective flow are the same as those in eqs. (28-31). The boundary conditions are given by:

Symmetric plane AE	$\partial u/\partial x = 0, \partial v/\partial x = 0, \partial T/\partial x = 0$	(36)
Right wall BC	$u = 0,\ v = 0,\ \partial T/\partial x = 0$	(37)
Right wall DF	$u = 0,\ v = 0,\ T = T_h$	(38)
Inlet Plane AB	$u = u_{in}, v = 0,\ T = T_{in}$	(39)
Step wall CD	$u = 0,\ v = 0,\ \partial T/\partial y = 0$	(40)
Outlet EF	$\partial u/\partial y = 0, \partial v/\partial y = 0, \partial T/\partial y = 0$	(41)

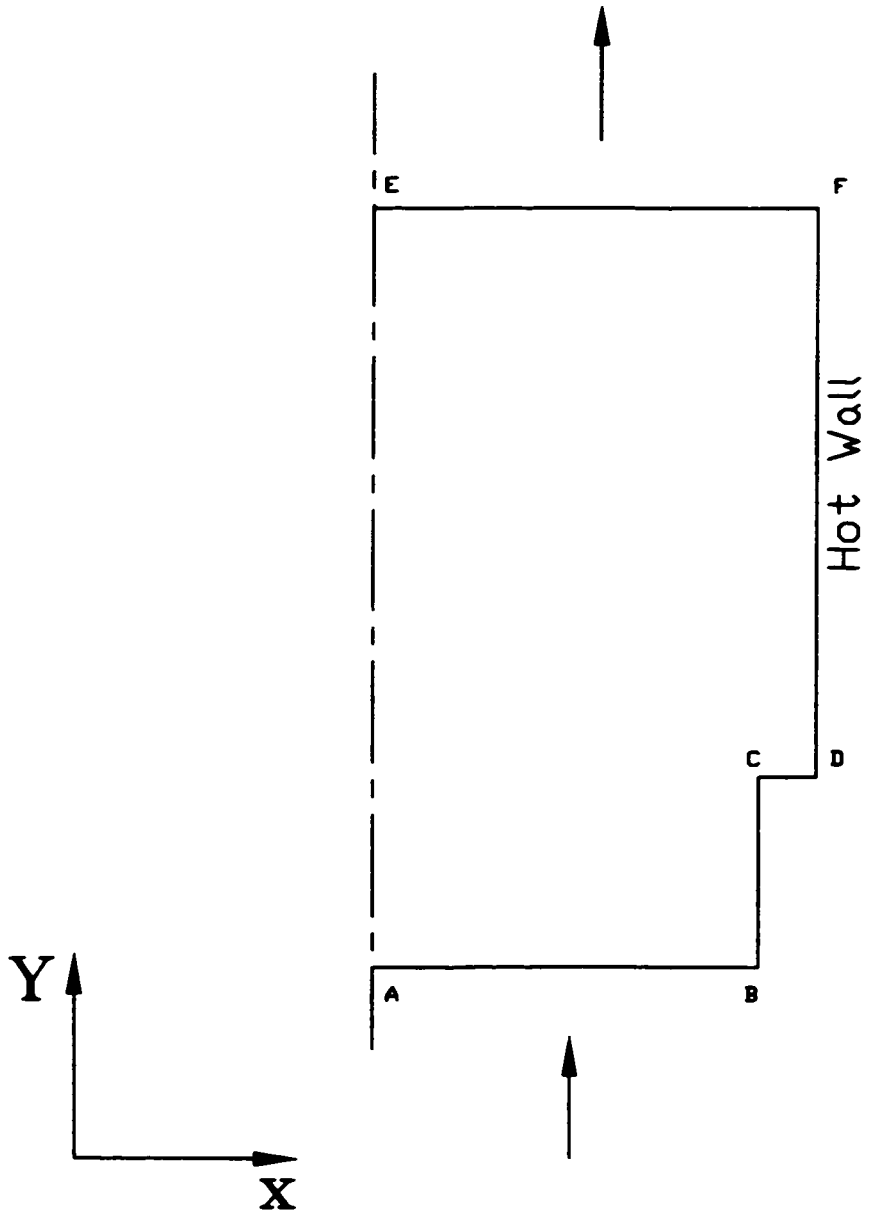

Fig. 8 Computation Domain for Test Case II

(The mixed convection problem behind a vertical backward facing step)

in the test cases,

DF = 167.4 mm , BC = 5.6 mm ;

EF = 10 mm, CD = 1.0 mm ;

T_{in} = 35°C , T_h = 65°C ;

The inlet air velocity u_{in} was set to different values to provide different Richardson numbers, R_i, as shown in Table 2.

where $R_i = G_r/R_e^2$ the Richardson number

$R_e = u\, l/\nu$ the Reynolds number

$G_r = g\beta\Delta T\, l^3/\nu^2 = 1.668 \cdot 10^7$ the Grashof number

The Richardson number represents the ratio of buoyancy force to inertial force. When it approaches infinity, the mixed convection flow becomes a natural convection flow, while Ri = 0 implies forced convection.

The computations were conducted using the same convergence criteria as before and the required iterations for different Richardson numbers were summarized in Table 3.

Table 3 Required Iterations for Test Case II

R_i	∞	100	10	1	0.1	0.01
SIMPLE	1640	1210	545	770	615	650
SIMPLET	1140	595	455	670	515	500

Figs. 9-10 show the temperature distribution plots for the cases of Richardson number equal to 100 and 0.01. When the Richardson number is equal to 100, the flow approaches natural convection flow. The heat transfer is weak and the temperature gradients near the hot wall are so small that the center of the channel can sense the hot wall. When the Richardson number equals to 0.01, the flow approaches forced convection flow. The heat transfer increases and the temperature gradients near the hot wall are much greater than for the case when the Richardson number is equal to 100. The center of the channel even cannot sense the existence of the hot wall. Fig. 10 also shows that the temperature gradient at the section of y = 0.006m is less than the ones at the sections of y = 0.02m and y = 0.05m. It implies that the point on the wall at y = 0.006m is in the recirculation zone caused by the backward facing step. The reattachment point moves downwards when the Richardson number increases.

Figs. 11 and 12 show the residual histories for Ri = ∞ and 100. It can be seen that when the Richardson number is large, indicating that buoyancy is the dominant factor driving the flow, the SIMPLET method provides faster convergence than SIMPLE. When the Richardson number is small, the number of iterations required for SIMPLET is only slightly less than that for SIMPLE and therefore, the faster convergence effect of SIMPLET becomes more moderate. As with the SIMPLER method [4], an extra equation (step 3 of solution procedure) must be solved in each iteration for SIMPLET. This extra computational work per iteration will increase the CPU time around 10% and offset the benefit obtained from a decrease in the number of iterations required.

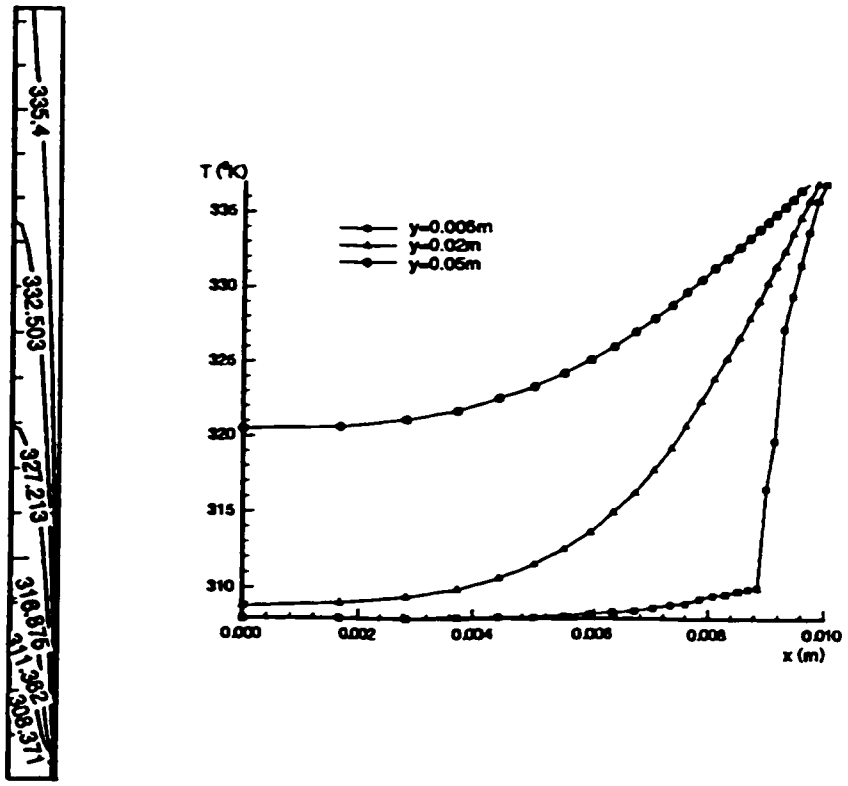

Fig. 9 Temperature Distribution (^{o}K) for the Test Case II (Ri = 100)

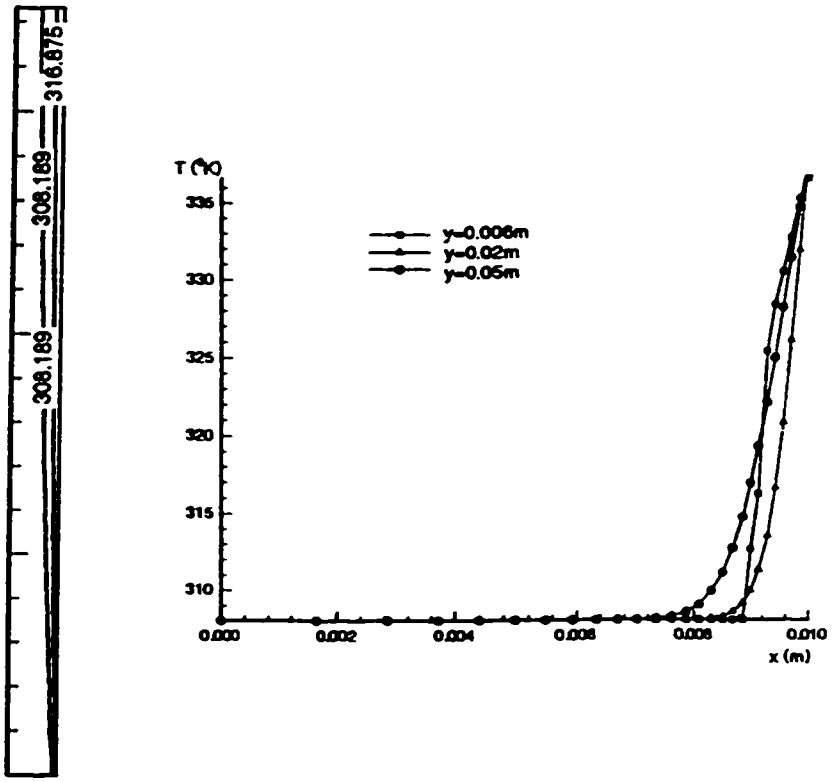

Fig. 10 Temperature Distribution (^{o}K) for the Test Case II (Ri = 0.01)

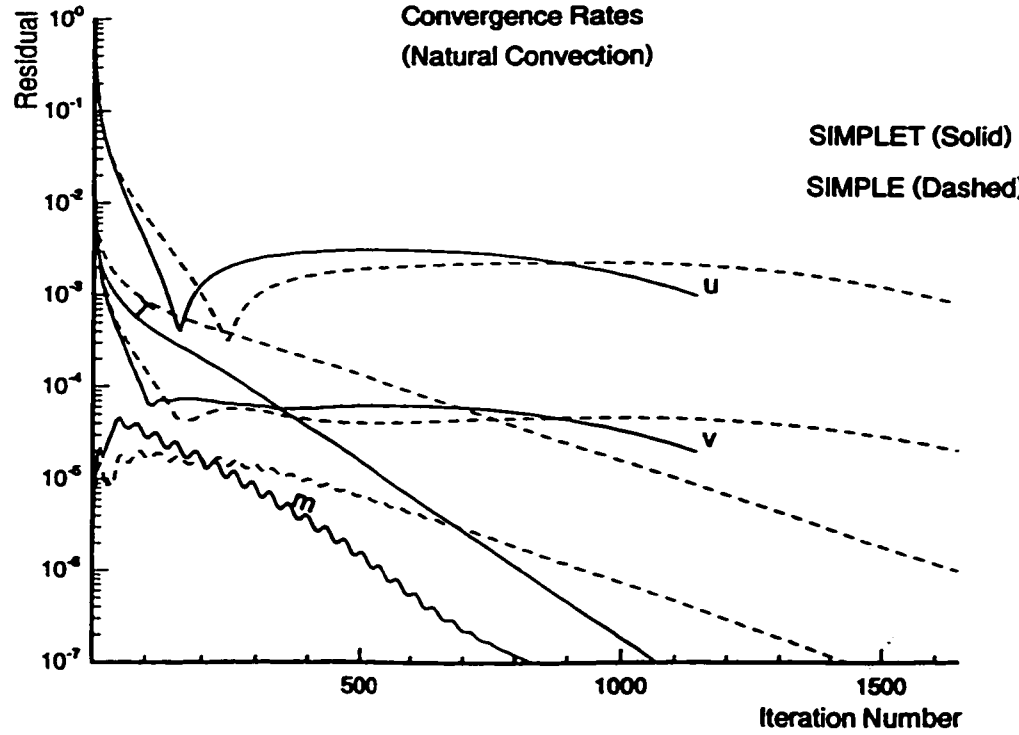

Fig. 11 Residual Histories for Test Case II (Ri = ∞)

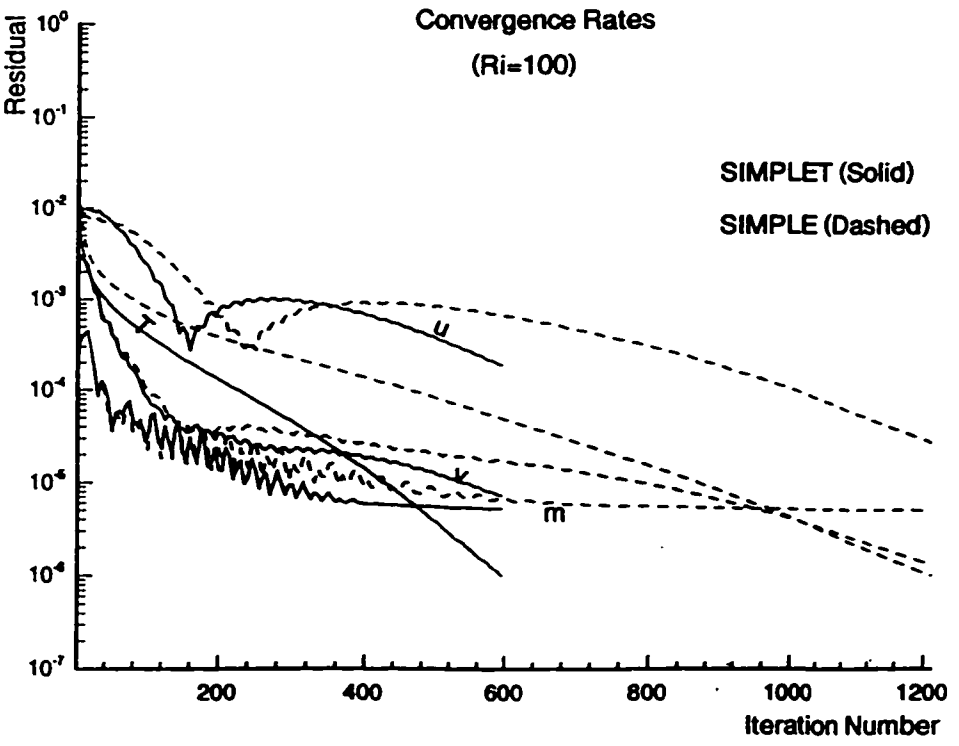

Fig. 12 Residual Histories for Test Case II (Ri = 100)

4.3 Summary

For laminar, buoyancy-driven flows, there is no direct link between velocity and temperature in the original momentum equations . The temperature influences the velocity indirectly through changes in the density. By introducing the Boussinesq approximation, a direct link between the velocity and temperature is established, and the temperature, T, is treated as an explicit variable in the discrete momentum equations. The introduction of the Boussinesq approximation makes it easier for the solution to reach convergence as shown in Fig. 2.

The SIMPLET algorithm was developed to make the direct link between velocity and temperature not only in the discrete momentum equations but also in the solution procedure. The derivation of the pressure linked equation considers that the velocity change is caused by both pressure changes and temperature changes. Therefore, the solution procedure is consistent and usually provides faster convergence.

The solution procedure is not the only factor that influences the convergence rate. The initial estimate and the under-relaxation factors are usually the major factors which influences the convergence rate. Therefore, no quantitative conclusion about the convergence rate can be drawn except when identical initial estimates and under-relaxation factors are used. This is universal for all algorithm development. In addition to that, the faster convergence benefit is usually conditional. For example, the SIMPLEC method usually provides faster convergence than SIMPLE does, but not always. Fig. 2(a) , for example, shows that SIMPLEC even provides a slightly slower convergence rate when compared with SIMPLE for this particular case. The CELS

method for natural convection flows usually provides faster convergence than the SIMPLE family of methods as shown in the figures of ref. [13], but not always. When the time step is small, the CELS method provides slower convergence than SIMPLER and SIMPLEC do as shown in Fig. 8 in ref. [13]. Compared with SIMPLE, when the pressure-velocity coupling is the factor mainly responsible for slow convergence, the SIMPLEC usually provides faster convergence[6]. In a similar fashion, when the temperature-velocity coupling is the factor mainly responsible for slow convergence, SIMPLET usually provides faster convergence than SIMPLE.

Like the development of SIMPLE itself and other modifications such as SIMPLER and SIMPLEC, the development of SIMPLET algorithm was done for a steady two-dimensional flow with staggered grids in a Cartesian coordinate system. This can be considered as its weakness. However, it is also its merit. For example, the SIMPLE method can be extended to collocated grid system instead of staggered grid system[3], the SIMPLET can then also be extended to collocated grid system without any special consideration since its development was exactly the same.

CHAPTER 5

THE APPLICATIONS OF SIMPLET TO TURBULENT BUOYANCY-DRIVEN FLOWS

The temperature variation in the flow fields encountered in modern electronic equipment and other industrial facilities is large enough that the flows with appreciable length scales are nearly always turbulent. As a preview to the application of the SIMPLET algorithm to real industrial problems, this thesis investigates several application cases of turbulent mixed convection flows in a cavity where the geometry is relatively complex and convex corners are involved.

5.1 The New Version of SIMPLET

When there are large temperature differences in the flow field, use of the Boussinesq approximation is not appropriate [19]. Based on the Boussinesq approximation, the buoyancy force is computed by $g\rho\beta(T - T_r) = gB(T - T_r)$, where g is gravity, $\beta = -(\partial\rho/\partial T)_p/\rho$ is the thermal expansion coefficient and T_r is the reference temperature. It is obvious that once the Boussinesq approximation is applied, the buoyancy force will not only depend on the temperature, but also on the reference temperature. How the reference temperature, T_r, is determined, is always a controversial issue. More than that, in order to keep the truncation error of determining the buoyancy

force to a certain level, the allowed temperature variation range is limited.

Fig. 13 shows the relative error of determining density caused by introducing the Boussinesq approximation for water at a reference temperature of $T_r = 50^oC$. It can be seen that the allowed temperature variation range is only $\pm 10^oC$ in order to keep the computational error in determining the buoyancy force less than 5%. Therefore, a new version of the Pressure Linked Equation which does not employ the Boussinesq approximation was developed.

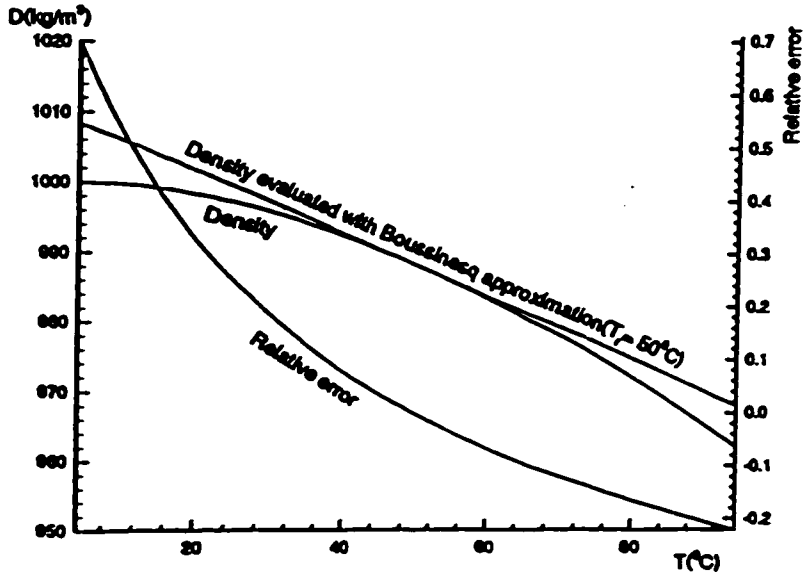

Fig. 13 Determination of Water Density With and Without the Boussinesq approximation

Introducing a density correction in a manner similar to velocity correction and pressure correction used previously gives:

$$\rho = \rho^{*} + \rho' \tag{42}$$

and noting that the velocity change is caused not only by a pressure change but also by a density change, an updated pressure linked equation can be developed in the following way.

By removing the Boussinesq approximation, eqs. (11'-23') can be rewritten as follows:

$$a_e u_e = \sum a_{nb} u_{nb} + b + (p_P - p_E) A_e + (\rho_P + \rho_E) g_x \Delta V/2 \tag{11''}$$

$$a_e u_e^{*} = \sum a_{nb} u_{nb}^{*} + b + (p_P^{*} - p_E^{*}) A_e + (\rho_P^{*} + \rho_E^{*})\, g_x \Delta V/2 \tag{12''}$$

$$a_e u_e' = \sum a_{nb} u_{nb}' + (p_P' - p_E') A_e + (\rho_P' + \rho_E') g_x \Delta V/2 \tag{15''}$$

$$u_e' = d_e (p_P' - p_E') + \delta_e (\rho_P' + \rho_E') \tag{16''}$$

where $d_e = A_e / a_e$ (17)

$$\delta_e = g_x \Delta V/(2\, a_e) \tag{17''}$$

so that, finally

$$u_e = u_e^{*} + d_e (p_P' - p_E') + \delta_e (\rho_P' + \rho_E') \tag{18a''}$$

Similarly,

$$u_w = u_w^{*} + d_w (p_W' - p_P') + \delta_w (\rho_W' + \rho_P') \tag{18b''}$$

$$v_n = v_n^{*} + d_n (p_P' - p_N') + \delta_n (\rho_P' + \rho_N') \tag{18c''}$$

$$v_s = v_s^{*} + d_s (p_S' - p_P') + \delta_s (\rho_S' + \rho_P') \tag{18d''}$$

The final pressure linked equation keeps the same form as before, as follows:

$$a_p p_P' = \sum a_{nb} p_{nb}' + b \qquad (20'')$$

where a_p , $\sum a_{nb}$, a_E , a_W , a_N , a_S are the same as in equations (21) and (22) and

$$b = c_W - c_E + c_S - c_N$$
$$+ [(\alpha_W - \alpha_E + \alpha_S - \alpha_N)\ \rho_P'$$
$$+ \alpha_W \rho_W' - \alpha_E \rho_E' + \alpha_S \rho_S' - \alpha_N \rho_N'] \qquad (23'')$$

where c_E , c_W , c_N , c_S $\alpha_E, \alpha_W, \alpha_N, \alpha_S$ are the same as in eq. (24) and eq. (27)

In the new version of the pressure linked equation for general cases, the density appears directly in the extra, square bracketed term.

It is obvious that nothing needs to be changed in the solution procedure except for the use of the new version of the pressure linked equation instead of the old one.

5.2 Turbulent Buoyancy-Driven Flow Test Cases

As mentioned in Chapter 4, the motivation of the SIMPLET algorithm development is not to improve the precision of the solution. The present modification does not change the final discrete algebraic equations. Therefore no precision issue is involved. The solutions using SIMPLE and SIMPLET are the same (as shown in chapter 4). The main purpose for the test cases is to show how the method is implemented and how much the convergence rate of the energy equation would be improved.

Fig.14 (a) shows a sketch of the test cavity to be studied in the present work. It represents a cavity which has been investigated experimentally quite extensively. It has a height of 297 mm, a width of 149 mm, and a depth of 48.5 mm. Water enters the horizontal inlet which has a height of 8 mm, a length of 203 mm and is incorporated into

the cavity at the top of the left vertical wall. A horizontal exit of the same size is connected at the bottom of the same vertical wall. All the walls are considered to be adiabatic except for the right vertical wall which is maintained at a uniform temperature using copper block heaters. This test cavity has been investigated in the heat transfer laboratory at McMaster University for several years. It was motivated by industrial applications and has its important applications to at least one company in Ontario. Two former Ph.D. students in our group also worked on it. Both experimental results and traditional numerical results are available in the thesis of G. Numberg. [20] My research is based on their experimental research efforts. The major conclusions from their thesis are:

1. Because the width of the model is not too great and the boundary along this direction is not insulated, a three dimensional effect exists. However, the flow still can be reasonably treated as a two dimensional near the mid-plane.

2. The inlet is long enough (l = 25d) to stabilize the flow entering the cavity. The perturbation caused by the water supply system (the pipe system, the instrument transducer location etc.) will not seriously affect the flow inside the cavity. A precise measurement of the velocity distribution profile and the turbulence level of the fluid at the section A-A' can therefore be avoided.

3. The flow inside the cavity is turbulent because of the flow separation in the cavity and the heat transfer from the hot wall, though the inlet Re number is lower than 1000. This will also be illustrated later.

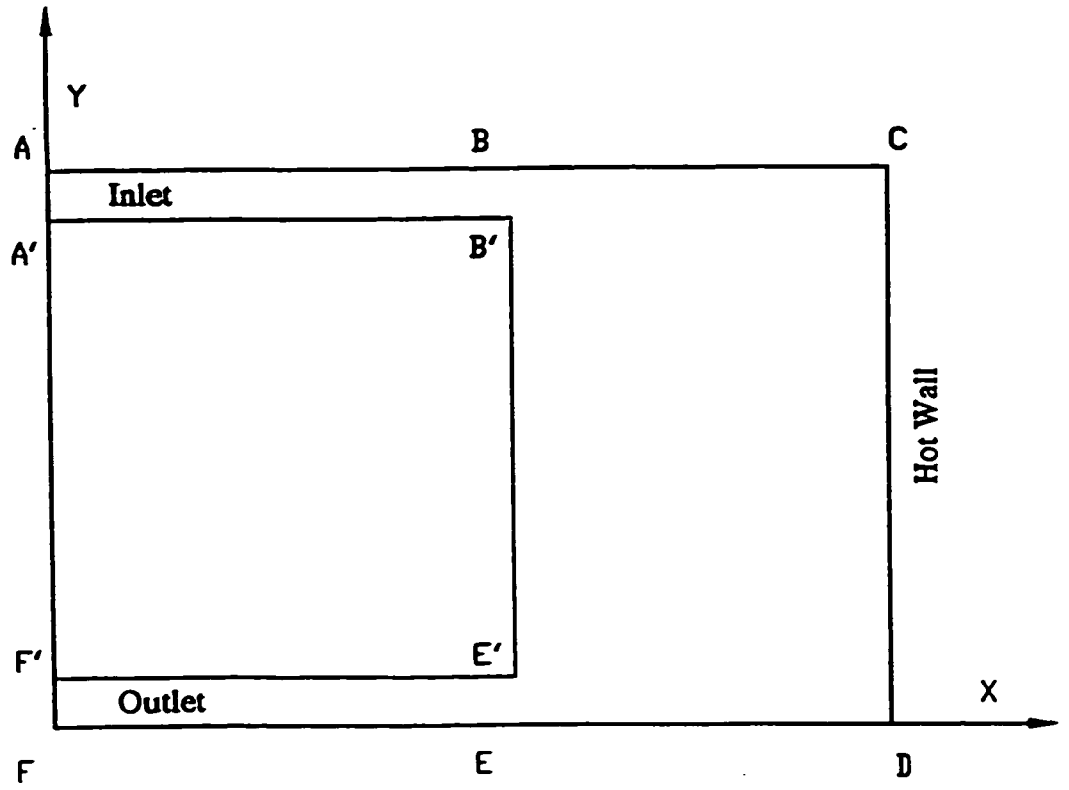

Fig 14 (a) Computational Domain of The Turbulent Flow Test Cavity

For all the test cases, the common boundary conditions are assigned as follows:

1) Constant temperature, T_{wr} , is maintained on the right wall. All other walls are assumed to be insulated and boundary fluxes are zero.

2) No slip conditions, $u = 0$, $v = 0$ are applied to all the walls.

3) Neumann conditions, $\partial\phi/\partial x = 0$, are prescribed at the outlet boundary for all the variables, ϕ.

The inlet conditions for u, v, T are prescribed to provide the three different test cases (see Table 4). The Grashof number and the Richardson number, Ri, are based on the height of the cavity. In all the test cases, the Grashof numbers are greater than $1.0 \cdot 10^9$. Therefore, the flow inside the cavity will be turbulent.[1] The Richardson number represents the ratio of buoyancy to inertial force. The importance of the buoyancy force increases in the order A, B, C.

Table 4 Summary of Test Cases

CASE	A	B	C
u (m/sec)	0.124	0.063	0.063
v (m/sec)	0	0	0
T (^{o}C)	22.3	24.0	25.9
T_{wr} (^{o}C)	42.5	63.0	80.6
Gr	$2.87 \cdot 10^9$	$10.7 \cdot 10^9$	$24.2 \cdot 10^9$
Ri	1.27	11.9	19.4

5.3 Turbulence Models

For turbulent flows, the main concern for engineers is not the details of turbulence behavior, but its time-averaged effects. The process of time-averaging, however, will introduce some statistical correlation terms involving fluctuating velocities U_i' and temperature (T') into the conservation equations. These terms can only be determined by turbulence models. Analogous to Newton's law of viscosity, Boussinesq [21] introduced a turbulent stress τ_t and a turbulent viscosity μ_t to model the Reynolds stress term, $\overline{U_i'U_j'}$, as follows:

$$\tau_t \equiv - \rho\overline{U_i'U_j'} = \mu_t \partial U_i/\partial x_j - 2/3\delta_{ij}\rho k \qquad (43)$$

When i is not equal to j, $\tau_t = \mu_t \partial U_i/\partial x_j$, which accounts for the shear stress due to turbulence motion, otherwise, $\tau_t = \mu_t \partial U_i/\partial x_i - 2/3\rho k$, which accounts for the normal stress due to turbulence motion, the counterpart of molecular motion being the static pressure term p/ρ. Unlike the molecular viscosity, the turbulent viscosity, μ_t, is not a property of the fluid but is a flow parameter dependent on the local turbulence. Its value usually varies from point to point within a given flow field. In a similar manner, the turbulent heat flux can be expressed as

$$-\overline{U_i'T'} = \alpha_t \partial T/\partial x_i = \nu_t/\sigma_t \partial T/\partial x_i \qquad (44)$$

where σ_t is the turbulent Prandtl number.

Once the turbulent viscosity concept is introduced, the governing equations can be rewritten as follows:

$$\partial U_j/\partial x_j = 0 \qquad (45)$$

$$\partial U_i/\partial t + U_j\, \partial U_i/\partial x_j = -1/\rho \partial/\partial x_i\, [p + 2k\rho/3\,] + \partial/\partial x_j\, [(\nu + \nu_t)\partial U_i/\partial x_j\,] + g_i \qquad (46)$$

$$\partial T/\partial t + U_j\, \partial T/\partial x_j = \partial/\partial x_j\, [(\alpha + \alpha_t)\partial T/\partial x_j] \qquad (47)$$

The introduction of turbulence viscosity, ν_t , provides a framework for constructing a turbulence model, but it does not constitute a model itself. The remaining task is to express the turbulent viscosity in terms of known or calculable quantities. The turbulence model equations for calculating the viscosity, ν_t , are part of the governing differential equations and therefore will significantly influence the flow field solution. For turbulent flows, the solution depends on the turbulence model being used.

5.3.1 The Standard k-ε, Two Equation Model

One of the most widely used turbulence models is the so-called k-ϵ, two equation model. The k is the notation for turbulent kinetic energy per unit mass, so $k^{1/2}$ describes turbulent velocity fluctuation strength. The ϵ is the rate of dissipation of turbulent kinetic energy. From dimensional arguments it can be shown that $\epsilon \sim u'^3/l$ where l is an integral length scale. Analogous to the evaluation of molecular viscosity from kinetic theory, the turbulent viscosity, $\nu_t = \mu_t/\rho \sim u'l$, can be expressed as:

$$\nu_t = C_\mu\, k^{1/2}\, k^{3/2}/\epsilon = C_\mu\, k^2/\epsilon \qquad (48)$$

where

C_μ is a constant coefficient

$k^{1/2}$ is the turbulent velocity fluctuation strength

$k^{3/2}/\epsilon$ is the turbulence length scale

The detailed derivation and modeling of the two equations for k and ε can be found in

[22]. The commonly used version of the k and ϵ equations are:

$$\partial k/\partial t + U_j\, \partial k/\partial x_j = \partial/\partial x_j\, [(\nu + \nu_t/\sigma_k)\partial k/\partial x_j] + \nu_t\, (\partial U_i/\partial x_j + \partial U_j/\partial x_i)\, \partial U_i/\partial x_j - \epsilon \tag{49}$$

$$\partial \epsilon/\partial t + U_j\, \partial \epsilon/\partial x_j = \partial/\partial x_j\, [(\nu + \nu_t/\sigma_\epsilon)\partial \epsilon/\partial x_j] + \nu_t\, C_1 \epsilon/k (\partial U_i/\partial x_j + \partial U_j/\partial x_i)\, \partial U_i/\partial x_j - C_2 \epsilon^2/k \tag{50}$$

where the commonly accepted values for the model constants are [23]:

$C_\mu = 0.09$

$C_1 = 1.44$

$C_2 = 1.92$

$\sigma_k = 1.0$

$\sigma_\epsilon = 1.3$

$\sigma_t = 0.9$

Owing to assumptions made in the modeling of the k and ϵ equations, this model is only valid for high turbulence Reynolds number, fully developed turbulent flows. It cannot be applied to the near wall region, where the local Reynolds number is low and the flow is not fully developed turbulent or may even be laminar. To solve this problem, an empirical or semi-empirical wall function is often used to assign values to the near wall grid points and thus exclude the near wall region from the application domain of the turbulence model. The wall function concept is to divide the near wall region into two sub-layers; the fully turbulent inertial sub-layer and the viscous sub-layer. In the fully turbulent inertial sub-layer, the velocity profile and temperature profile are assumed to follow a universal semi-empirical logarithmic velocity profile and

temperature profile determined experimentally. It is further assumed that the production and dissipation of turbulent energy balance and the Prandtl's mixing length model holds. In the viscous sub-layer, turbulence can be neglected. The detailed wall function treatment can be found in [24].

5.3.2 The Modified k-ε, Two Equation Models

In order to use the standard k-ϵ two equation model in wall bounded flows, a suitable wall function must be provided by experiment in advance. A standard wall function was designed for plane wall with zero curvature and zero pressure gradient along the wall. Its application is limited. More than that, in certain cases, such as in recirculating flows, no suitable wall function can be determined. Then, the standard k-ϵ two equation model must be abandoned. The buoyancy- driven flow dealt with in this test cavity belongs to such a case. There are many modified k-ϵ two equation models developed by different investigators for solving different problems, mostly for separated flow problems. In order not to use the wall function, some extra terms or coefficients are introduced into the k, and ϵ equations and the ν_t expression to modify the model so that the updated model can be used in the whole computational domain including near wall regions where the local Reynolds number is low and the flow is laminar or in the transition regime. For this reason, these modified k-ϵ, two equation models are usually referred to as low Reynolds number k-ϵ, two equation models. The general form of these models can be expressed as follows.

$$\partial k/\partial t + U_j\, \partial k/\partial x_j = \partial/\partial x_j\, [(\nu + \nu_t/\sigma_k)\partial k/\partial x_j] + \nu_t\, (\partial U_i/\partial x_j + \partial U_j/\partial x_i)\, \partial U_i/\partial x_j - \epsilon \qquad (49')$$

$$\partial(\epsilon - D)/\partial t + U_j\, \partial(\epsilon - D)/\partial x_j = \partial/\partial x_j\, [(\nu + \nu_t/\sigma_\epsilon)\partial(\epsilon - D)/\partial x_j] + \nu_t\, C_1\, f_1\, (\epsilon - D)/k(\partial U_i/\partial x_j + \partial U_j/\partial x_i)\, \partial U_i/\partial x_j - C_2\, f_2\, (\epsilon - D)^2/k + E \qquad (50')$$

$$\nu_t = C_\mu\, f_\mu\, k^2/\epsilon \qquad (48')$$

The damping functions (f_1, f_2, f_μ) and extra coefficients are summarized in Table 5 from a number of researchers.

Table 5 The Modified k-ε Two Equation Models

Model	Conventional	Lam-Bremhorst[25] (Neumann)	Lam-Bremhorst [25] (Dirichlet)
ϵ_w	Wall Function	$\partial\epsilon/\partial y = 0$	$\nu\partial^2 k/\partial^2 y$
C_μ	0.09	0.09	0.09
C_1	1.44	1.44	1.44
C_2	1.92	1.92	1.92
σ_k	1.0	1.0	1.0
σ_ϵ	1.3	1.3	1.3
f_μ	1.0	$[1- \exp(-0.0165R_k)]^2 \cdot(1 + 20.5/R_t)$	$[1- \exp(-0.0165R_k)]^2 \cdot(1 + 20.5/R_t)$
f_1	1.0	$1.0 + (0.05/ f_\mu)^3$	$1.0 + (0.05/ f_\mu)^3$
f_2	1.0	$1.0 - 0.3 \exp(-R_t^2)$	$1.0 - \exp(-R_t^2)$
D	0	0	0
E	0	0	0

Table 5 Continued

Model	Hassid-Poreh [26]	Hoffman [27]	Launder-Sharma [28]
ϵ_w	0	0	0
C_μ	0.09	0.09	0.09
C_1	1.45	1.81	1.44
C_2	2.0	2.0	1.92
σ_k	1.0	2.0	1.0
σ_ϵ	1.3	3.0	1.3
f_μ	$1 - \exp(-0.015R_t)$	$\exp[-1.75/(1 + R_t/50)]$	$\exp[-3.4/(1 + R_t/50)^2]$
f_1	1.0	1.0	1.0
f_2	$1.0 - 0.3 \exp(-R_t^2)$	$1.0 - 0.3 \exp(-R_t^2)$	$1.0 - \exp(-R_t^2)$
D	$2\nu k/y^2$	$\nu/y\ \partial k/\partial y$	$-2\nu(\partial k^{1/2}/\partial y)^2$
E	$-2\nu(\partial k^{1/2}/\partial y)^2$	0	$2\nu\nu_t(\partial^2 u_i/\partial^2 x_j)^2$

Table 5 Continued

Model	Dutoya-Michard [29]	Chien [30]	Reynolds [31]
ϵ_w	0	0	$\nu\partial^2 k/\partial^2 y$
C_μ	0.09	0.09	0.084
C_1	1.35	1.35	1.0
C_2	2.0	1.8	1.83
σ_k	0.9	1.0	1.09
σ_ϵ	0.95	1.3	1.3
f_μ	$1 - 0.86 \exp[-(R_t/600)^2]$	$1 - \exp(-0.0115y^+)$	$1- \exp(-0.0198R_t)$
f_1	$1 - 0.04[-(R_t/50)^2]$	1.0	1.0
f_2	$1.0 - 0.3 \exp[-(R_t/50)^2]$	$1.0 - 0.22 \exp[-(R_t/6)^2]$	$\{1.0 - 0.3 \exp[-(R_t/3)^2]\}/f_\mu$
D	$2\nu(\partial k^{1/2}/\partial y)^2$	$2\nu k/y^2$	0
E	$-C_2 f_2 \epsilon D/k$	$-2\epsilon\nu/y^2\exp(-0.5y^+)$	0

Table 5 Continued

Model	Nagano-Hishida [32]	H.G.G.G [33]	To-Humphrey [34]
ϵ_w	0	$\partial\epsilon/\partial y = 0$	$2\nu(\partial k^{1/2}/\partial y)^2$
C_μ	0.09	0.09	0.09
C_1	1.45	1.44	1.44
C_2	1.9	1.92	1.92
σ_k	1.0	1.0	1.0
σ_ϵ	1.3	1.3	1.3
f_μ	$1 - \exp(-y^+/26.5)$	$[1- \exp(-0.0066R_t)]^2\cdot[1+500 \exp(-0.0055 R_t)/R_t]$	$\exp[-2.5/(1 + R_t/50)]$
f_1	1.0	$1.0 + (0.05/ f_\mu)^3$	1.0
f_2	$1.0- 0.3 \exp(-R_t^2)$	$1.0 - 0.3/[1-0.7 \exp(-R_k)] \cdot \exp(-R_t^2)$	$[1.0 - 0.3\exp(-R_t^2)]\cdot f$ If $y^+ > 5$, $f = 1$; if $y^+ < 1$, $f = 1.0-\exp(-R_t^2)$
D	$2\nu(\partial k^{1/2}/\partial y)^2$	0	0
E	$(1- f_\mu)\nu\nu_t(\partial^2 u_i/\partial^2 x_j)^2$	0	0

5.3.3 Turbulence Models for Buoyancy-Driven Flows

By introducing the Boussinesq approximation, there is an extra term, $\beta g_i (T - T_r)$, in the momentum equation for buoyancy-driven flows. Handling this extra term in a similar manner to the other terms in the momentum equation to derive the k, and ϵ equations means there will be an extra term, $- \beta g_i \nu_t / \sigma_t \, \partial T/\partial x_i$, in the k equation and an extra term, $- C_3 \epsilon/k \beta g_i \nu_t / \sigma_t \, \partial T/\partial x_i$, in the ϵ equation. Different approaches have been put forward for determining the coefficients C_3, $C_3 = C_1$ [35] or $C_3 = 0.7$ [36] or $C_3 = \tanh |v/u|$ [34].

Considering a heated vertical wall, a large source of the buoyancy-induced turbulence production occurs in a relatively small temperature gradient along the vertical direction. The term, $- \beta g_i \nu_t / \sigma_t \, \partial T/\partial x_i$ in the k and ϵ equations cannot reflect this behavior correctly. Daly and Harlow presented the generalized gradient diffusion hypothesis (GGDH) [38] to replace the modeling of velocity temperature correlation (also see [39], [36],[40]).

Even adding the above mentioned extra terms, the standard k-ε, two equation model and the modified k-ε, two equation models still cannot simulate the turbulent mixed convection flow well [41]. The difficulty comes from various aspects. In natural convection, the transition from laminar to turbulent flow occurs at relatively high Rayleigh numbers and in most cases, the molecular effects and turbulent-molecular interactions remain significant in some regions of the flow field while others are fully turbulent. In certain cases, even at very high Rayleigh numbers, turbulence may be confined to only some regions of the flow domain [41]. The velocity distribution near a

wall does not follow a universal rule. In the case of natural convection over a horizontal heated surface, turbulence occurs instantly as soon as the Rayleigh number exceeds a critical value. The velocity close to the wall is very low or has a value of zero. For a wall-jet like boundary layer along a heated vertical wall, the velocity exhibits a sharp peak very close to the wall [41]. For the flows near to the vertical non-adiabatic surfaces, George and Capp [42] identified an inner layer and an outer layer, separated by the position of maximum velocity. The inner layer can be further divided into two sub-layers. [42] In summary, turbulence modeling for buoyancy driven flows is difficult and buoyant flows are known to exhibit features which cannot easily be described by statistical averaging. Detailed information about this section can be found in [41], [42].

5.3.4 The RNG Turbulence Model

The RNG (RENORMALIZATION GROUP) turbulence model has received much attention in the years since it was first presented in 1986 [43]. It uses the following expression for the effective viscosity, μ_{eff}, to account for the low Reynolds number effect

$$\nu_{eff} = \nu_l \{1.0 + k\,[C_\mu/(\nu_l\,\varepsilon)]^{1/2}\}^2 \qquad (51)$$

The k and ε equations for the RNG model are:

$$\partial(\rho k)/\partial t + \partial(\rho U_i k)/\partial x_i = \partial/\partial x_i[\alpha_k \mu_{eff}\,(\partial k/\partial x_i)] + G_k + G_b - \rho\varepsilon \qquad (49'')$$

$$\partial(\rho\varepsilon)/\partial t + \partial(\rho U_i \varepsilon)/\partial x_i = \partial/\partial x_i[\alpha_\varepsilon \mu_{eff}\,(\partial\varepsilon/\partial x_i)] + C_{1\varepsilon}\,\varepsilon/k[G_k + (1 - C_{3\varepsilon})\,G_b] - C_{2\varepsilon}^{*}\,\rho\varepsilon^2/k \qquad (50'')$$

where G_k is the production of turbulence kinetic energy due to velocity gradients:

$$G_k = \mu_t S^2 \qquad (52)$$

$$S = (2S_{ij} S_{ij})^{1/2} \tag{53}$$

$$S_{ij} = (\partial U_j / \partial x_i + \partial U_i / \partial x_j)/2 \tag{54}$$

G_b is the production of of turbulence kinetic energy due to buoyancy:

$$G_b = - g_i \alpha \mu_t / \rho \, \partial \rho / \partial x_i \tag{55}$$

α is determined by the following implicit formula

$$| (\alpha - 1.3929)/(\alpha_l - 1.3929)|^{0.6321} | (\alpha + 2.3929)/(\alpha_l + 2.3929)|^{0.3679} = \mu_l / \mu_{eff} \tag{56}$$

$$\alpha_l = 1/Pr = k_f /(\mu C_p) \tag{57}$$

$$C_{2\varepsilon}^{*} = C_{2\varepsilon} + [C_\mu \eta^3 (1 - \eta/\eta_0)]/(1 + \beta\eta^3) \tag{58}$$

$$\eta = Sk/\varepsilon \tag{59}$$

$$\eta_0 = 4.38$$

$$\beta = 0.012$$

Coefficients take the following values:

$$C_\mu = 0.0845$$

$$C_{1\varepsilon} = 1.42$$

$$C_{2\varepsilon} = 1.68$$

$$C_{3\varepsilon} = 0.8$$

$\alpha_k = \alpha_\varepsilon$ are determined by the following implicit formula

$$| (\alpha - 1.3929)/(1.0 - 1.3929)|^{0.6321} | (\alpha + 2.3929)/(1.0 + 2.3929)|^{0.3679} = \mu_l / \mu_{eff} \tag{60}$$

The RNG energy equation is

$$\partial(\rho T)/\partial t + \partial(\rho U_i T)/\partial x_i = \partial/\partial x_i[\alpha \mu_{eff} (\partial T/\partial x_i)] \quad (61)$$

where the Prandtl number, α, is determined by the following implicit formula

$$| (\alpha - 1.3929)/(\alpha_l - 1.3929)|^{0.6321} | (\alpha + 2.3929)/(\alpha_l + 2.3929)|^{0.3679} = \mu_l/\mu_{eff} \quad (62)$$

$$\alpha_l = 1/Pr = k_f/(\mu_l C_p) \quad (63)$$

It can be seen that the low Reynolds number effect is also considered through the treatment of turbulent Prandtl numbers in equations for k, ε, and T (α_k, α_ε, α) as a function of μ_t/μ_{eff}. A rate of strain term R in eq. 58 is introduced to capture the sensitivity of turbulence to flows with streamline curvature to make the model suitable for flows with massive separation and anisotropic large-scale eddies.

$$R = [C_\mu \eta^3 (1 - \eta/\eta_0)]/(1 + \beta\eta^3)\, \varepsilon^2/k \quad (64)$$

The RNG model is being accepted by more and more researchers and has become one of the three turbulence model choices in the FLUENT software, the industry standard.

5.3.5 Other Turbulence Models

In the early stages of turbulence model development, zero equation and one equation models played an important role but they are too simple to be applied in the test cases under study. A detailed review of these models is given in [20,23]. In addition to the k-ϵ two equation model, there are some other two equation models such as the k-ω model, where ω stands for the square of the fluctuating vorticity [22].

Most turbulence models are based on the concept of a turbulence viscosity. However, this concept is not always acceptable, especially for certain heat transfer

problems [44,45]. There are many other methods such as differential or algebraic Reynolds stress turbulence models to model Reynolds stress and turbulent heat transfer. Theoretically, these models can predict flow fields more precisely. However, the many coefficients involved in these models cannot be determined analytically and must be evaluated experimentally. Also, these coefficients are usually not universal but field dependent. Therefore, their applications are not as promising as at first sight. Detailed reviews of these models can be found in [46], [47].

5.3.6 Closing Remarks

Turbulence modeling is a very complex topic that has not yet reached maturity. The development of all the turbulence models are partly based on experimental results. Any modification to them without experimental support is therefore suspect. Natural convection is extremely sensitive to changes in the container configuration and the imposed boundary conditions so that the use of results from "similar" problems is dangerous [48]. Since no experimental research was involved in this thesis project, no modification to the turbulence model being used is introduced in the present study.

Different turbulence models fit different flow fields and there is not a perfect model for every flow. As far as precision and computation cost are concerned, the best model is field dependent. For the test cavity under study, the exit duct is at the same side of the cavity and the flux cross sections change suddenly at B-B' and E-E'. There should be at least four small separation zones at the corner of C, D, E' and B'. The convection caused by the buoyancy also leads to flow separation somewhere in the

cavity. These local separation zones can create turbulence. Besides, when the temperature difference between the right wall and the fluid is high enough, the buoyancy also promotes turbulence. [1] Therefore, even when the entering water velocity is as low as 0.124m/sec and the entrance duct Reynolds number is lower than 1000, the flow is still turbulent in the cavity. However, unlike ordinary high Reynolds number turbulent flow, the turbulence inside the cavity is usually not fully developed and somewhere near the wall, molecular viscosity cannot be neglected. Besides, there are rapid strain and streamline curvature regions in the recirculation zones. Based on this preliminary flow field analysis, the standard k-ε two equation model will not be considered for use.

Various low-Reynolds number k-ε two equation models have been used to simulate buoyancy-driven flows. Modifications are introduced to the empirical constants and the damping functions that are a function of normal distance to the wall. Obviously, the normal distance to the wall will jump around any convex corner in the computational domain and will cause a discontinuity problem.

In the newest version of the RNG turbulence model, a new variable, the distance to the nearest wall, is introduced to replace the normal distance to the wall to avoid the discontinuity problem [16]. Though the RNG turbulence model is also a semi-empirical model, compared with the other two equation k- ε models, it has better theoretical foundations (cf. [43]). It has also been tested for various cases and been applied to commercial software. The statement in the FLUENT users guide document that ".....All the features listed above make the RNG k-ε model more accurate and reliable for a wide class of flows than the standard k-ε model....." (cf. Ref 16, PP.6-21) shows that this

model is worth recommending though it is not perfect. Therefore, the RNG turbulence model is used in the present study.

It is claimed that the RNG turbulence model can be applied to the whole computational domain without a near wall treatment as most low Re-number models do. However, there is no reason to reject the use of a wall treatment when the RNG turbulence model is used. The FLUENT software also offer this option for use. In the current work, the near wall treatment is introduced with a two-layer model as follows, [16].

First, a Reynolds number based on distance from a wall is defined

$$Re_y = \rho k^{1/2} y / \mu_l \tag{65}$$

where y is the normal distance to the nearest wall

$$y = \min ||r - r_w|| \tag{66}$$

r is the position vector at the field point

r_w is the position vector at the wall point $r_w \in \Gamma_w$

Γ_w is the union of all the wall boundaries involved.

When $Re_y > 200$; the k- ε equation are solved to find μ_t and μ_{eff} as usual.

When $Re_y \leq 200$; the molecular viscosity plays an important role in this near wall region and a one equation model is used to determine μ_t :

$$\mu_t = \rho C_\mu k^{1/2} l_\mu \tag{67}$$

where k is solved by the k differential equation and l_μ is given by an algebraic equation as follows:

$$l_\mu = C_l\, y\, [1.0 - \exp(-Re_y / A_\mu)] \tag{68}$$

$$A_\mu = 70$$

$$C_l = \kappa C_\mu^{-3/4} \tag{69}$$

$$\kappa = 0.42$$

$$\varepsilon = k^{3/2}/l_\varepsilon \tag{70}$$

$$l_\varepsilon = C_l\, y\, [1.0 - \exp(-Re_y / A_\varepsilon)] \tag{71}$$

$$A_\varepsilon = 2C_l \tag{72}$$

5.4 Numerical Test

Computation was carried out on the Cray C-90 Supercomputer at San Diego Supercomputer Center. Coding by the author was initiated using the standard k-ε turbulence model with course grids and then an increased number of grid nodes was used to confirm that the solution was grid independent. When the RNG turbulence model with a two-layer model wall treatment was used, a denser grid distribution compared to that used in the standard k-ε model was necessary in the regions near the walls.

5.4.1 Code Development

The code development was based on the one developed for laminar flows in chapter 4. The RNG turbulence model was introduced into the code. The boundary conditions were clearly stated in section 5.2 except for the turbulence kinetic energy, k and the dissipation rate, ε. In fact, there should be no turbulence at the entrance of the

inlet, because the Reynolds number there is very low. The turbulence in the inlet is caused by the sudden cross-sectional area change at the entrance to the cavity and the recirculation inside the cavity. The natural convection inside the cavity also creates turbulence when the Rayleigh number is high. The turbulence in the inlet is caused by the downstream disturbance only and therefore is very weak. The turbulence kinetic energy, k, at the entry to the inlet (section A-A') is small. Since there are no experimental results available for setting the inlet condition of k, and ε in the present computations, the inlet condition is set as usual for turbulent conduit flows, ie.

$k_{in} = 0.01 \cdot 3u_{in}^2/2$

$\varepsilon_{in} = k_{in}^{3/2}/ d_{hy}$ where d_{hy} is the hydraulic diameter of the inlet section.

This assumption is acceptable for the following reasons:

1. A certain level of turbulence in front of the inlet always exists except in a well designed water tunnel which is not the case here.

2. Since inlet length is over 25d long and the Re number is less than 1000, the flow will laminarize. Therefore, the flow at the exit section of the inlet channel (B-B') is almost laminar whatever the turbulence level is in front of the inlet. (That is the reason why there is a long narrow inlet in front of the cavity.) It is not necessary to precisely measure and assign the turbulence level at the entry to the inlet (A-A').

3. Numerical experiments showed that there was not much difference when the inlet turbulence kinetic energy was increased by ten times or decreased to a tenth of the original value. The temperature distribution profile and velocity vector plots show no noticeable dependence on the inlet boundary conditions for k and ε.

The coefficients $\alpha_k = \alpha_\varepsilon = \alpha$ introduced in the k and ε equations of the RNG turbulence model are determined by the following implicit formula:

$$|(\alpha - 1.3929)/(1.0 - 1.3929)|^{0.6321} \, |(\alpha + 2.3929)/(1.0 + 2.3929)|^{0.3679} = \mu_l/\mu_{eff}$$

The coefficient, α, introduced in the energy equation, when the RNG turbulence model is used, is determined by the following implicit formula:

$$|(\alpha - 1.3929)/(\alpha_l - 1.3929)|^{0.6321} \, |(\alpha + 2.3929)/(\alpha_l + 2.3929)|^{0.3679} = \mu_l/\mu_{eff}$$

where $\alpha_l = 1/Pr = k_f/(\mu_l C_p)$

The determination of these coefficients should be conducted for every grid point and every iteration. When the Newton bisection method is used for this purpose, the computer code for determining these coefficients cannot be vectorized, and thus it will be computationally costly. In addition to that, all the model constants in turbulence models, including the other model constants in RNG, are of three digits accuracy only, therefore it is acceptable to simplify the determination of α. In this work, the following approximation formula for determining α was used to keep its value to a precision of three digital only.

$$\begin{aligned}\alpha = {} & C_1/[\ln(\mu_{eff}/\mu_l)]^6 + C_2/[\ln(\mu_{eff}/\mu_l)]^5 + C_3/[\ln(\mu_{eff}/\mu_l)]^4 + C_4/[\ln(\mu_{eff}/\mu_l)]^3 \\ & + C_5/[\ln(\mu_{eff}/\mu_l)]^2 + C_6/[\ln(\mu_{eff}/\mu_l)] + C_7 + C_8[\ln(\mu_{eff}/\mu_l)] \\ & + C_9[\ln(\mu_{eff}/\mu_l)]^2 + C_{10}[\ln(\mu_{eff}/\mu_l)]^3 + C_{11}[\ln(\mu_{eff}/\mu_l)]^4 + C_{12}[\ln(\mu_{eff}/\mu_l)]^5 \\ & + C_{13}[\ln(\mu_{eff}/\mu_l)]^6 \end{aligned} \qquad (73)$$

where the coefficients C_i , $i = 1, 13$ are determined once for a given Prandtl number by a separate subroutine instead of solving the implicit equation. The whole

variation range of μ_{eff}/μ_l should be divided into several sections so that the computational error will be controlled to the level of $1.0 \cdot 10^{-3}$. For the range of Prandtl number in the present study, 4-6 sections were sufficient to satisfy this demand.

5.4.2 Numerical results of the Field Behaviors

All the test cases were solved using both the SIMPLE and SIMPLET methods. As expected, the final velocity and temperature results are independent of the algorithm used.

Fig. 14 (b) shows the contour plot of the ratio of the turbulent viscosity to the molecular viscosity for the typical test case, case B. It can be seen that the flow inside the cavity is turbulent and that the turbulence in some regions is very weak. This makes the simulation difficult since no turbulence model is totally adequate for this kind of flow. A precise numerical prediction is nearly impossible.

Fig. 15 shows the numerically predicted velocity vector plots for the three test cases. From these plots it can be seen that the flow field in the cavity can be considered to be composed of two parts: one is the pressure-driven flow entering from the left inlet duct and turning downward and then exiting from the left exit duct; the other is the buoyancy driven flow moving up along the hot wall caused by the temperature difference between the right hot wall and the fluid.

In test case A, the mean kinetic energy of the entering flow is relatively high and the temperature difference between the right wall and the fluid is low. The main flow can reach the right wall and turn downward along the wall. The buoyancy-driven force

causes the flow near the right wall to move upward. Since the buoyancy is relatively weak, this second flow soon meets the main flow and separates from the hot wall to form a recirculation zone as shown in Fig. 15 (a). With a decrease in the entering flow mean kinetic energy and increasing buoyancy driving force due to the temperature difference between the right wall and the fluid, the separation point moves upward and the recirculation zone becomes larger as shown in Fig. 15 (b) for test case B. With a further increase in the buoyancy- driving force, the second flow caused by buoyancy is strong enough to reach the top wall then turn left. In contrast, the entering flow from the inlet is relatively weak, and after meeting the second flow, it separates from the top wall before it reaches the right wall. The flows interact with each other and then exit the cavity. The interactions between these two flows include momentum exchange and heat exchange. This is the case shown in Fig. 15 (c) for test case C. Figs. 16 show the corresponding velocity vector plots (on a coarser grid) obtained by experiment using LDA (Laser Doppler Anemometer) measurements for the three test cases A, B and C [20]. It can be seen by comparing figures 15 and 16 for comparable cases that the numerical results and the experimental results are in qualitative agreement.

More computations were conducted to support the preceding analysis. Fig. 17 contains the velocity vector plots for test case A where the inlet velocity was decreased from 0.124m/sec to 0.094 m/sec and 0.063 m/sec respectively. As expected, the recirculation-zone size increases and the separation point moves up the heated wall with decreasing inlet mean flow kinetic energy.

Figs. 18-20 show the numerical and experimental (from ref. [20]) temperature

distributions near the hot vertical wall at three different locations: y_l = 80 mm, y_m= 140 mm and y_h = 200 mm. It can be seen that there are large temperature gradients along the normal direction to the hot wall and the temperature profile soon levels off in the region away from the wall. Numerical simulations are in good agreement with the experimental data.

By comparing the results of case A and C provided by Nurnberg [20] using the standard k-ε turbulence model , the Lam and Bremhorst [25] low Reynolds number model and the results provided in this thesis using the RNG turbulence model, it can be seen that in these two cases, both the Lam and Bramhorst low Reynolds number model and the RNG turbulence model provide qualitative agreement with experimental results. However, in case B, where the two driving forces caused by pressure gradient and temperature gradient are nearly in balance, only the RNG turbulence model provides qualitative agreement. Fig. 21 shows the direct comparison of velocity vector plots between experimental results [20] and the numerical results using the three different turbulence models mentioned above. The most difficult case to simulate is mixed convection flow where the two driving forces caused by pressure gradient and temperature gradient are nearly in balance. In such a case, the advantage of the RNG turbulence model over other models becomes apparent.

5.4.3 Convergence Criteria and Algorithm

Due to the use of the RNG turbulence model and the two-layer model wall treatment, the underrelaxation factors for the present turbulent flow test cases are very

low. In the present work, the under relaxation factor for u, v, k, are at the level of 0.01 and different from case to case but kept the same when the SIMPLE and SIMPLET algorithms were used. The number of iterations required for convergence is much larger when compared to the cases using the standard k-ε turbulence model with wall function.

In turbulent flows, the interaction between the turbulence model and the momentum equations is usually the factor mainly responsible for slow convergence and the convergence rates of k, ε, u and v are the determinants in reaching a solution if the convergence criteria set in FLUENT [16] are used (ie. the normalized residual of temperature be less than $1.0 \cdot 10^{-6}$ and the normalized residuals of other variables less than $1.0 \cdot 10^{-3}$). Therefore, any of the SIMPLE family of algorithms does not show dramatic advantages over the simplest scheme, SIMPLE [49]. Figs. 22-24 show the residual history plots of u, v, m, T, k, and ε for the three test cases – case A, B and C respectively. For the sake of clarity, the figures for residual histories in turbulent flows are created for every 100 iterations. In order to make sure no misunderstanding is introduced, when parts of the plots are confusing, detailed residual history files were created for clarification. For case A , serious oscillations occur but suddenly disappear after 35000 iterations. The detailed residual histories of the variables using both SIMPLE and SIMPLET were created for each iteration. Fig. 25 shows the residual histories and the detailed oscillation situations.

It can be seen that the SIMPLET method usually provides a faster convergence rate than SIMPLE for temperature, but the convergence rates for achieving a solution are almost the same when SIMPLE and SIMPLET are used. However, in certain cases,

such as in test case B, where the driving forces are nearly in balance, the convergence rate of T is the determinant in reaching a solution. Here the SIMPLET method does provide faster convergence and the advantage of the SIMPLET algorithm becomes apparent. In fact, it is difficult to reach a converged solution using the SIMPLE algorithm at all if the requirements on the normalized residuals given above for all the variables are strictly satisfied. While a converged solution was reached after 25000 iterations using SIMPLET; after 40000 iterations, the residual of energy equation is still $2.0 \cdot 10^{-6}$ and no converged solution can be reached when SIMPLE was used.

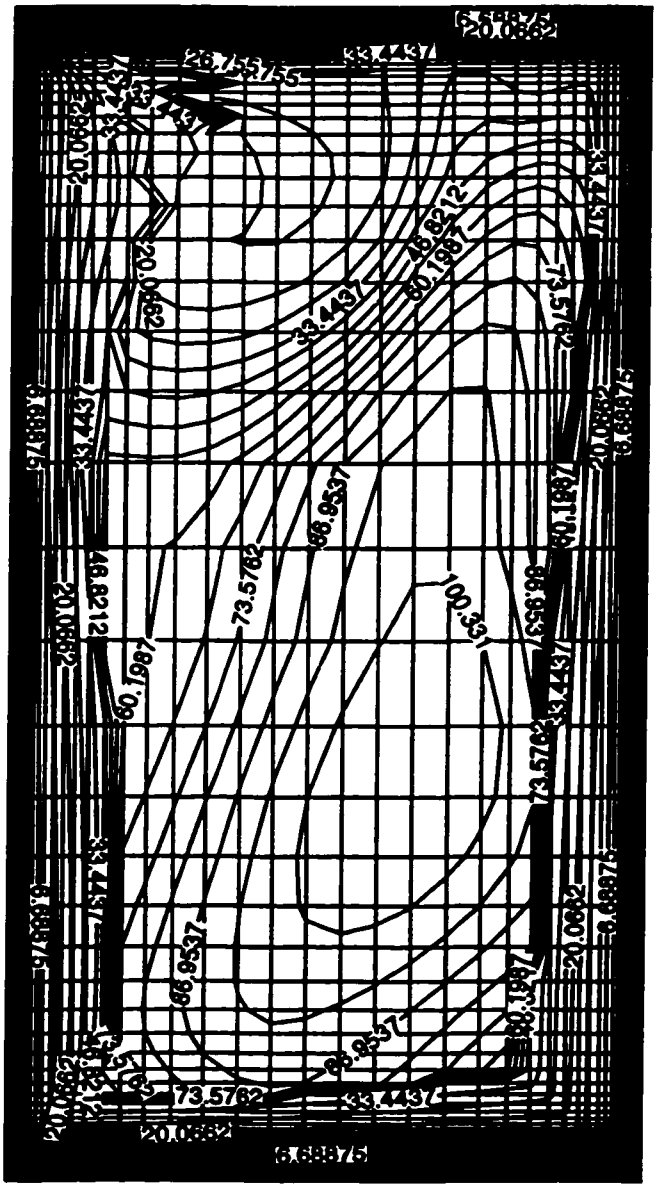

Fig. 14 (b) Non-dimensional Turbulence Viscosity (μ_t/μ_l) Distribution (Case B)

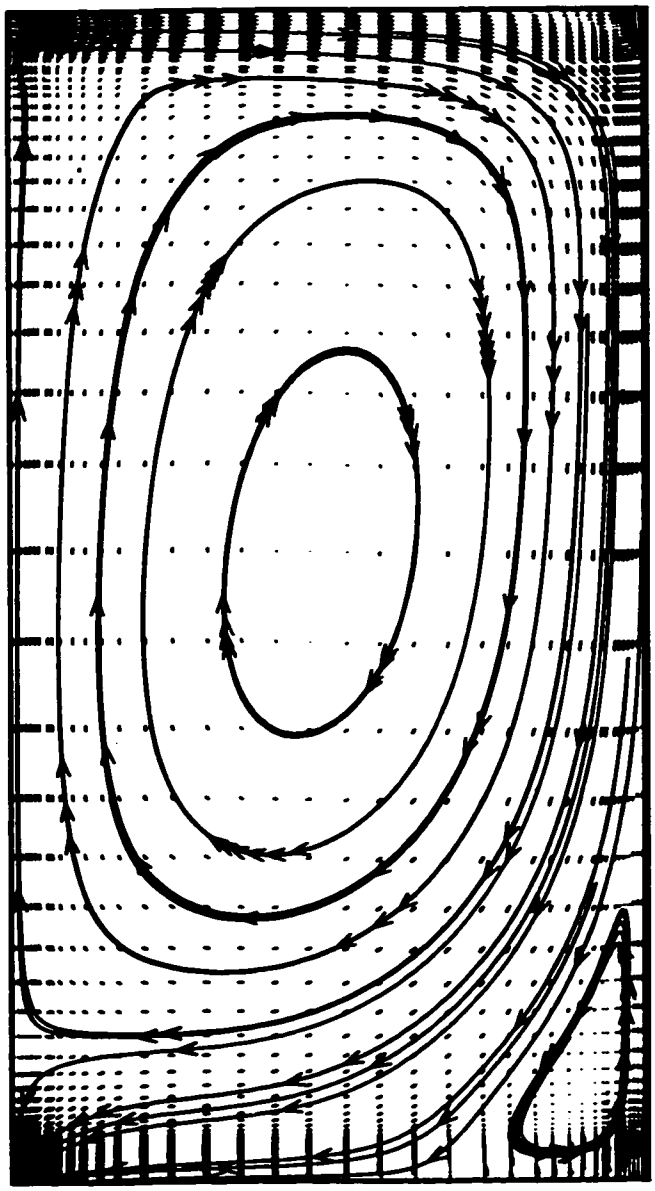

Fig. 15 (a) Numerical Prediction of Velocity Vector (Case A)

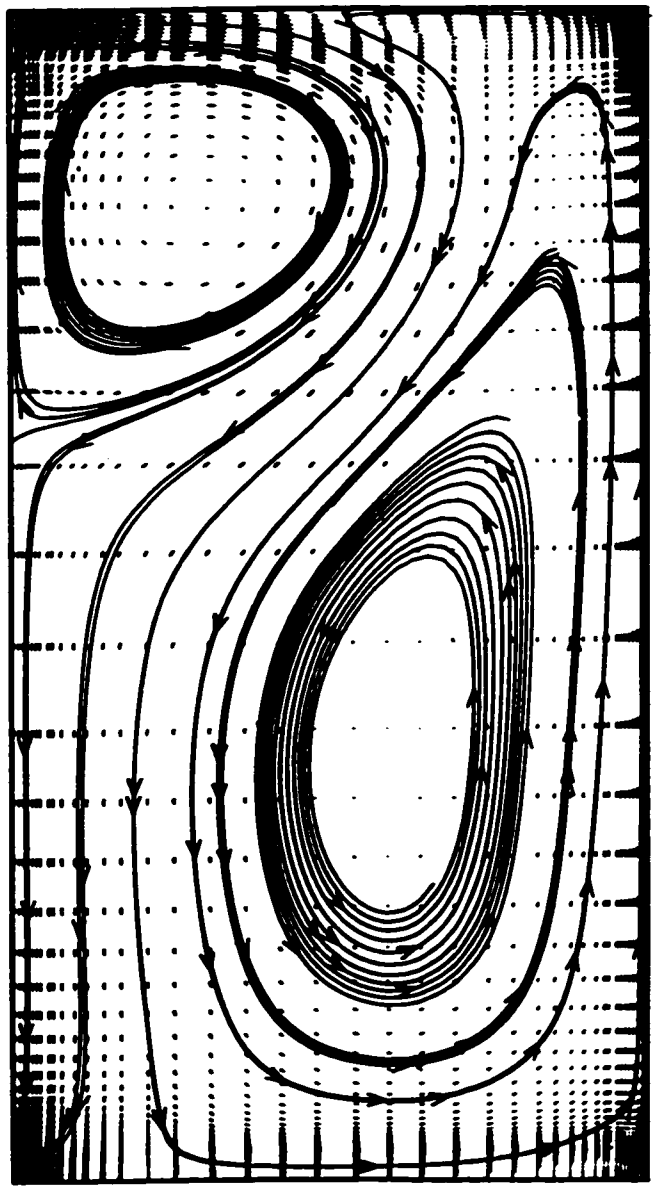

Fig. 15 (b) Numerical Prediction of Velocity Vector (Case B)

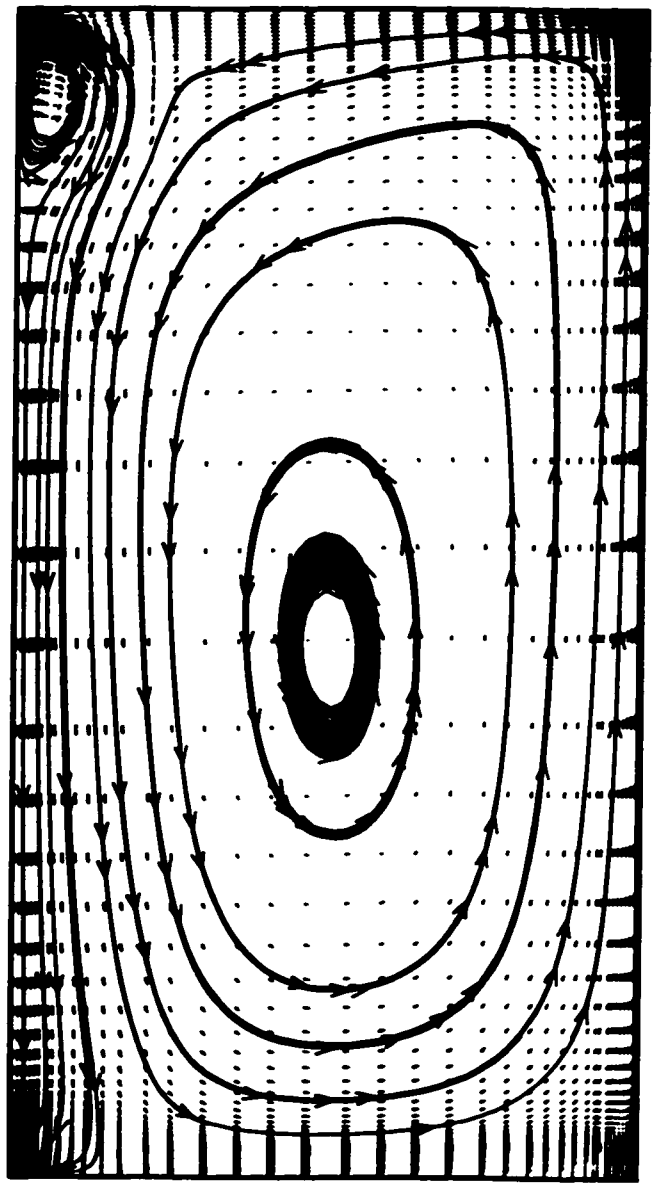

Fig. 15 (c) Numerical Prediction of Velocity Vector (Case C)

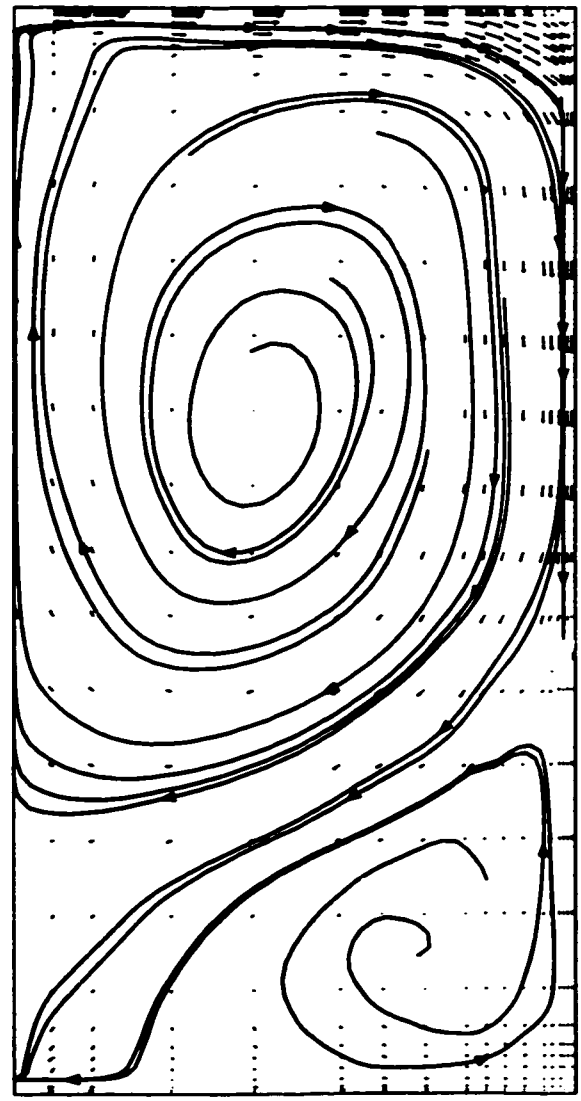

Fig. 16 (a) Experimental Results of Velocity Vector by LDA (Case A)

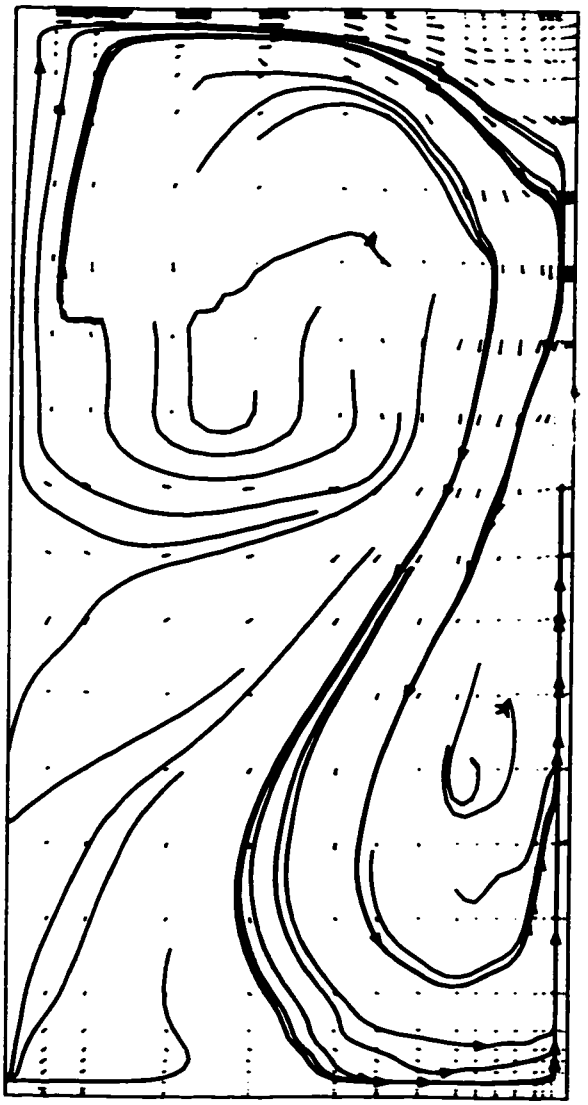

Fig. 16 (b) Experimental Results of Velocity Vector by LDA (Case B)

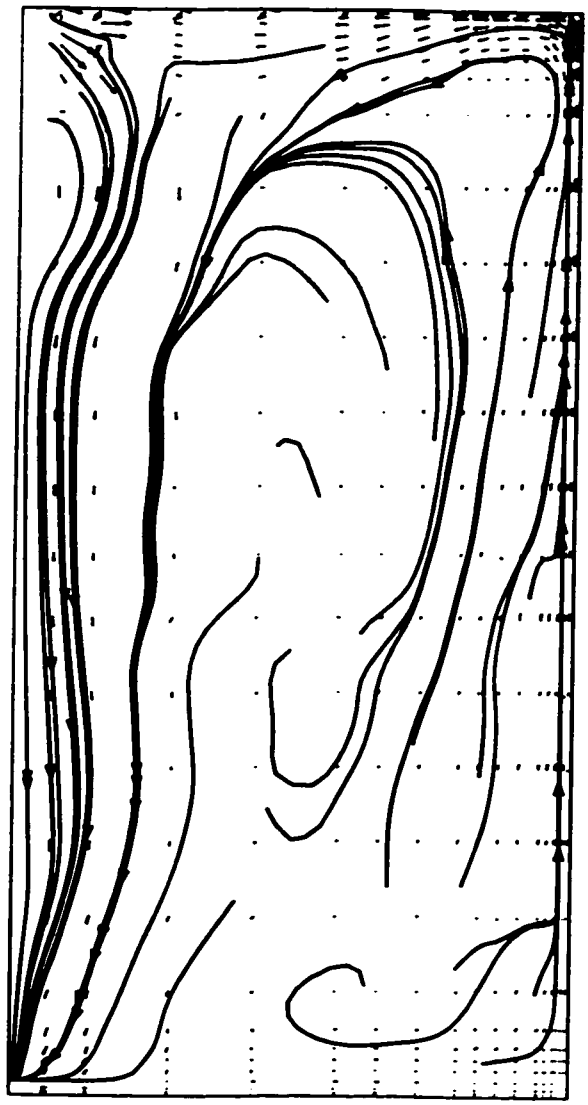

Fig. 16 (c) Experimental Results of Velocity Vector by LDA (Case C)

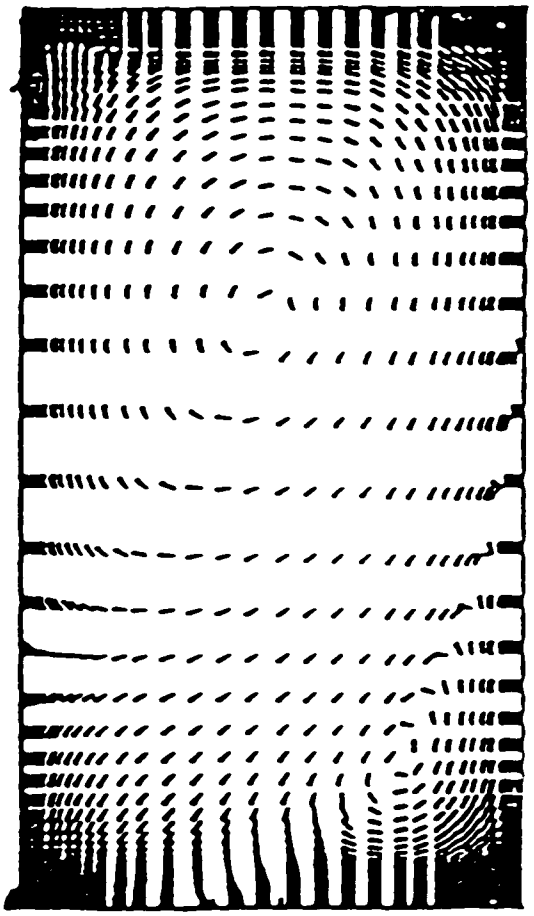

Fig. 17 (a) Numerical Prediction of Velocity Vector (Case A with u_{in} = 0.094 m/sec)

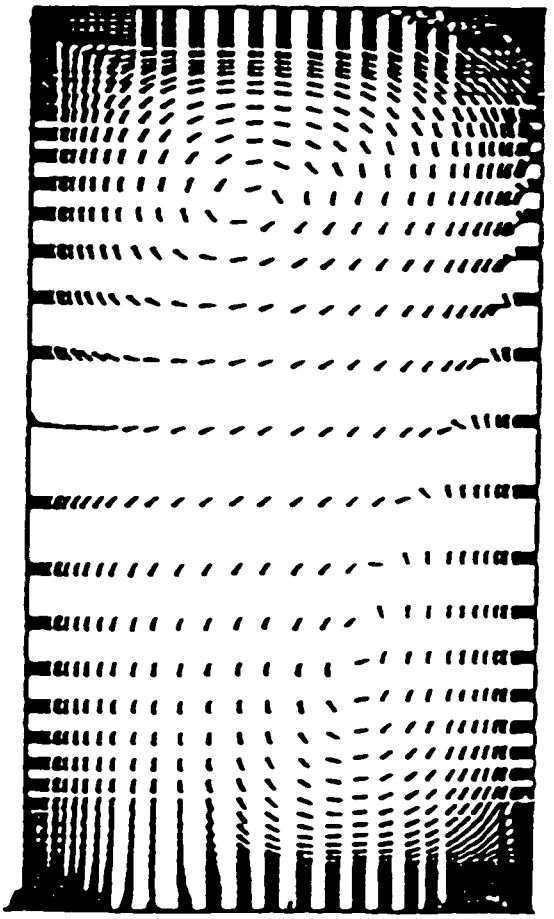

Fig. 17 (b) Numerical Prediction of Velocity Vector (Case A with $u_{in} = 0.063$ m/sec)

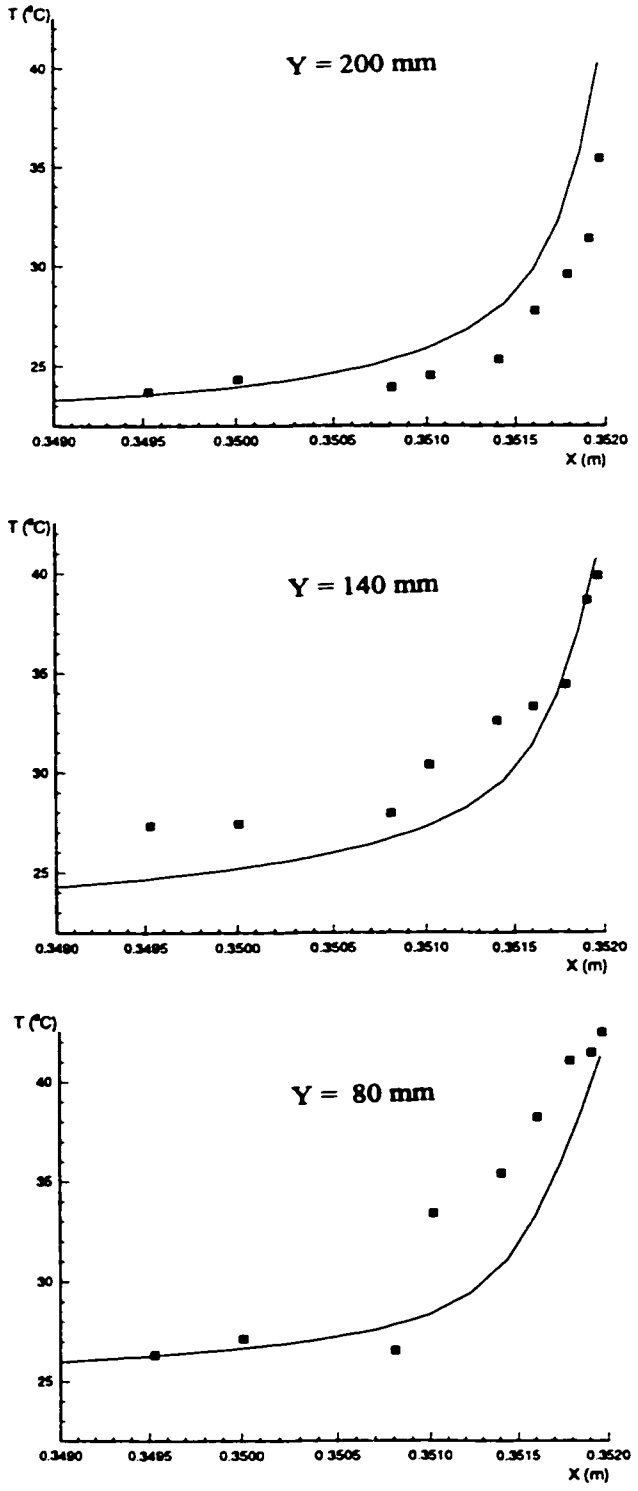

Fig. 18 Temperature Distribution Near the Hot Vertical Wall (Case A)

(Numerical Results ——— Experimental Results • [20])

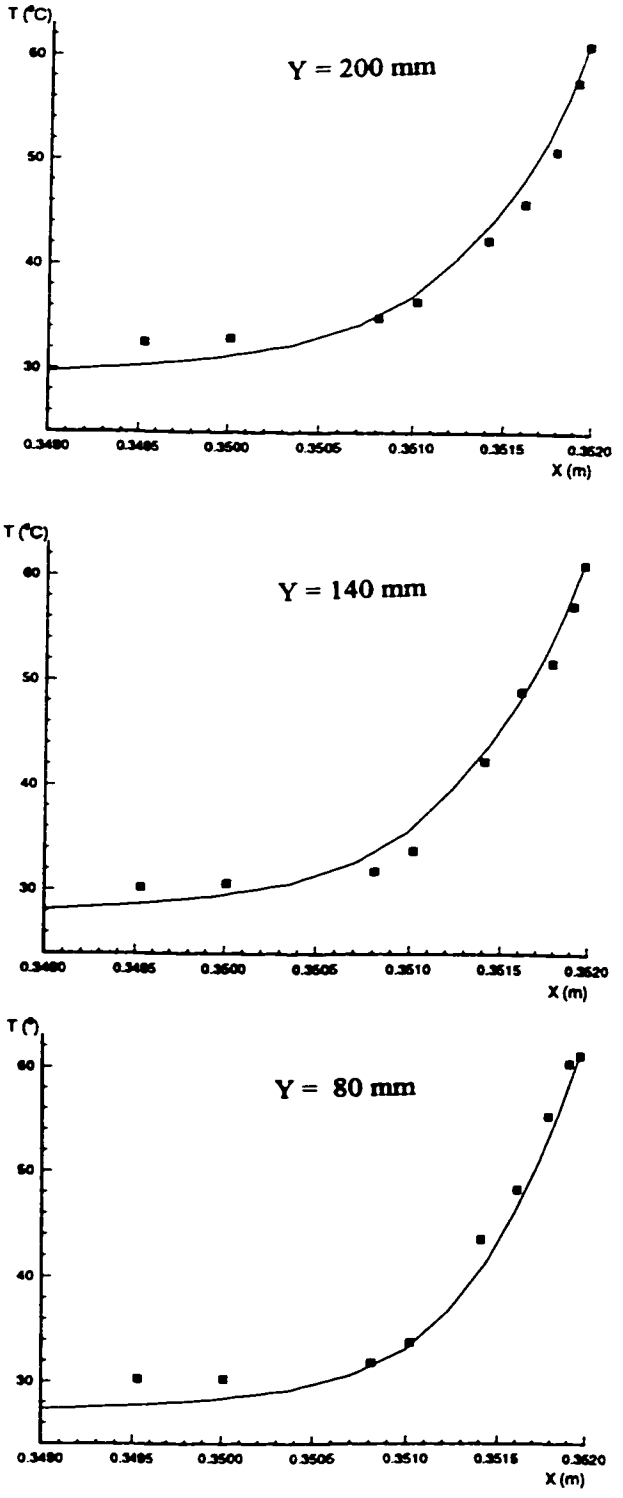

Fig. 19 Temperature Distribution Near the Hot Vertical Wall (Case B)

(Numerical Results ——— Experimental Results • [20])

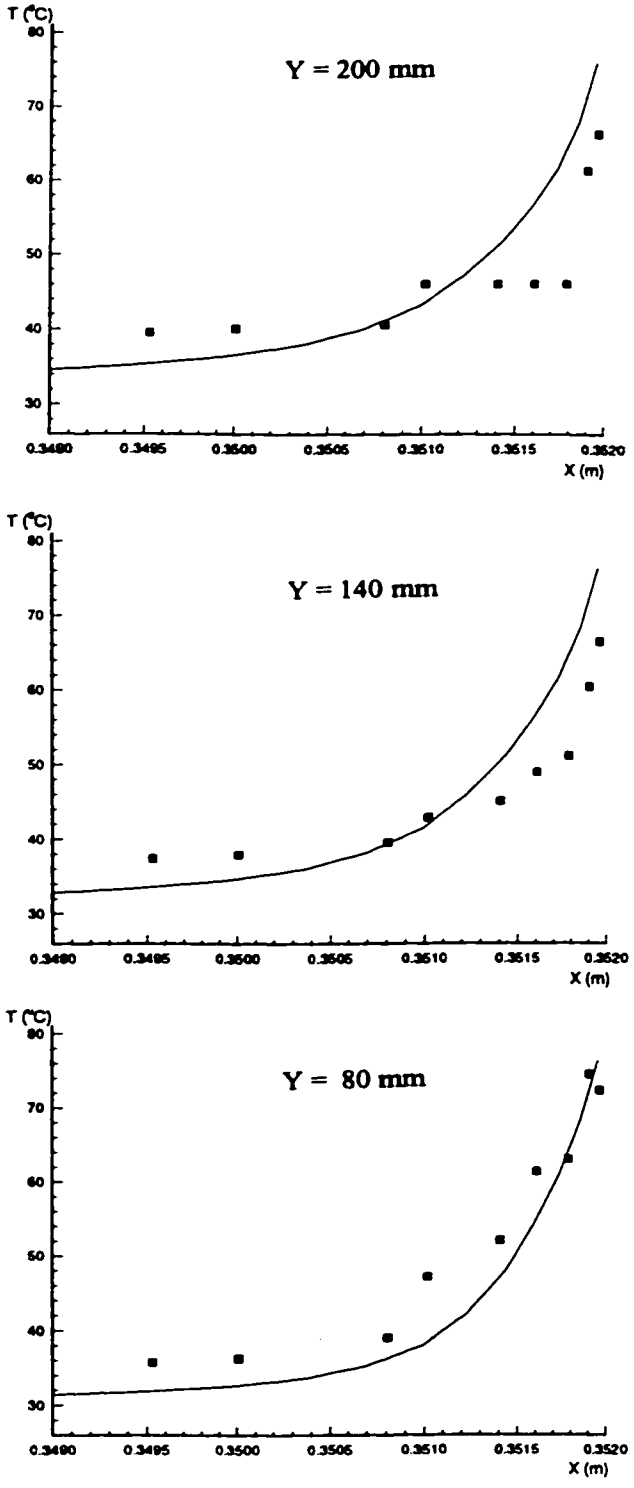

Fig. 20 Temperature Distribution Near the Hot Vertical Wall (Case C)

(Numerical Results ——— Experimental Results • [20])

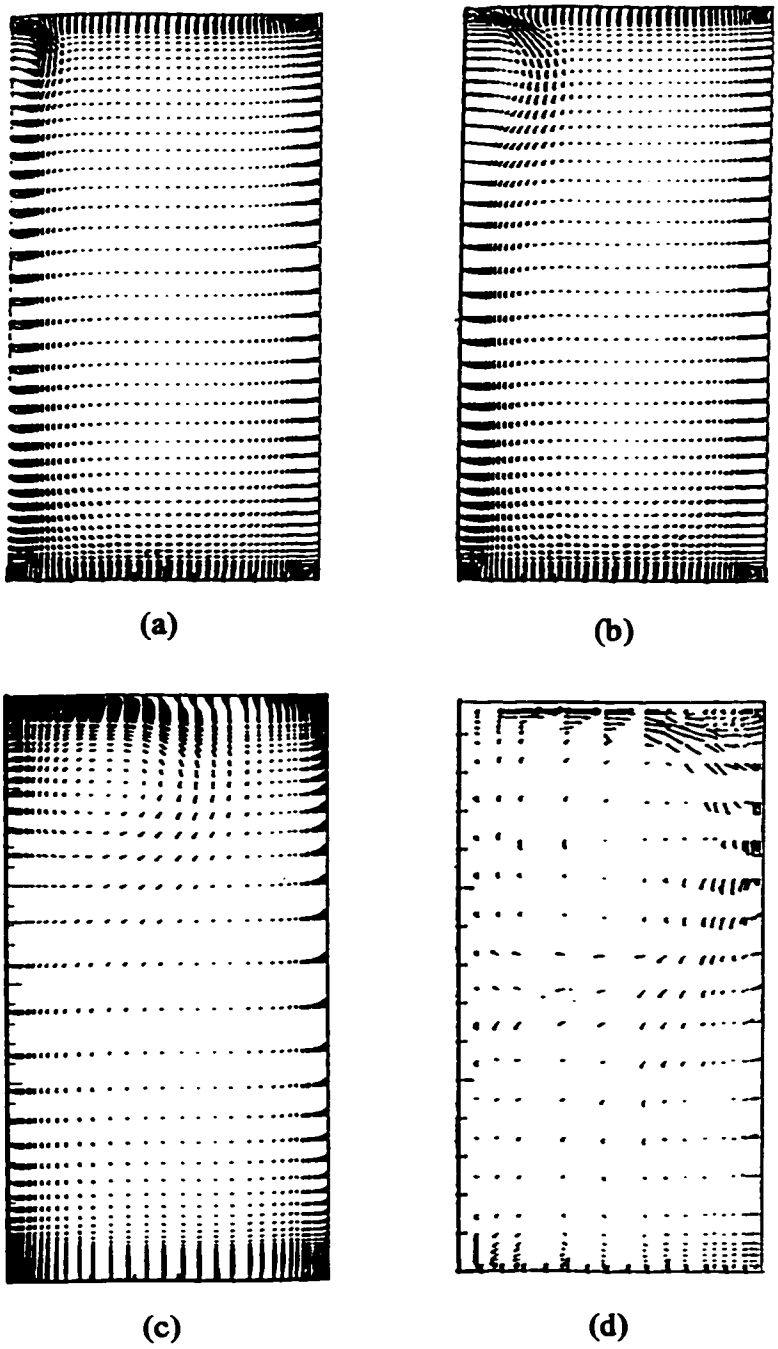

Fig. 21 Comparison of Different Turbulence Model Predictions For Case B

(a) k-ε Turbulence Model[20]; (b) Lam and Bramhorst Low Reynolds Number Turbulence Model [20]; (c) the RNG Turbulence Model;

(d) LDA Experimental Results [20].

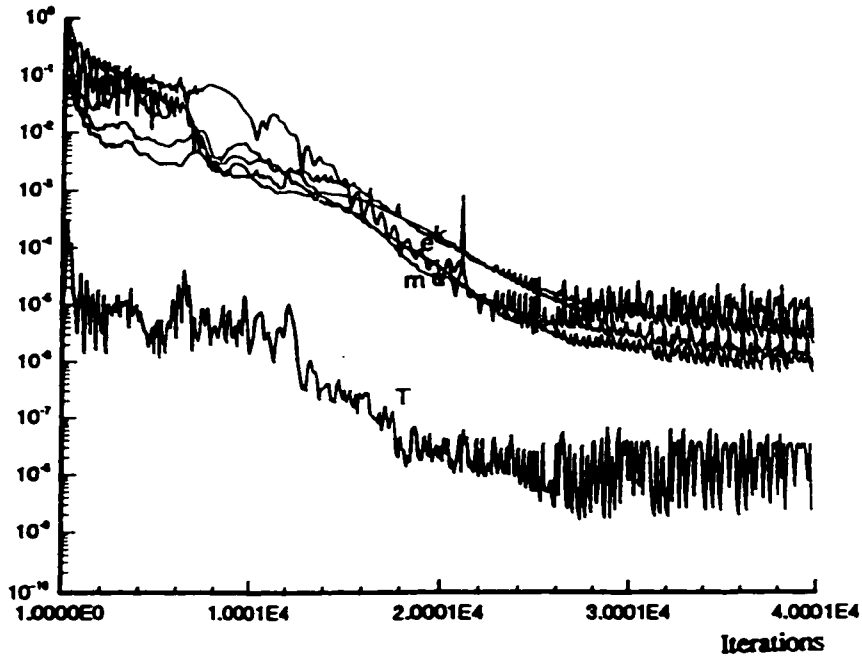

Fig. 22 (a) Residual Histories For Case A Using SIMPLE

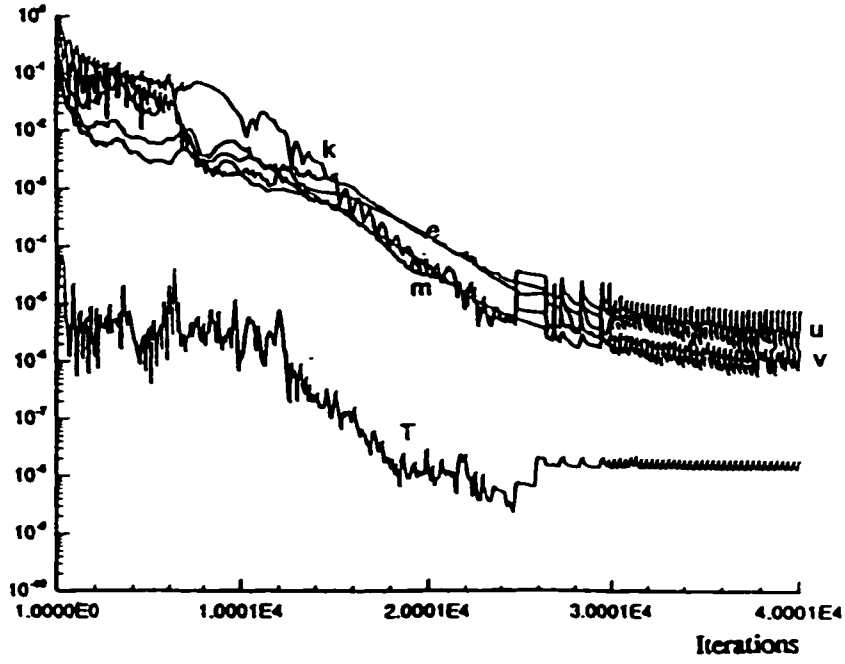

Fig. 22 (b) Residual Histories For Case A Using SIMPLET

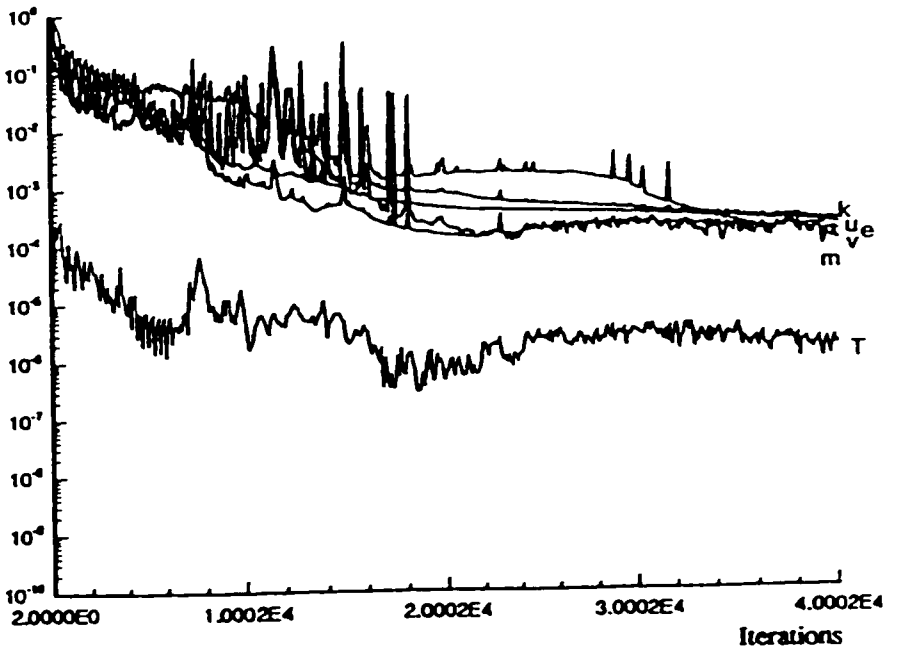

Fig. 23 (a) Residual Histories For Case B Using SIMPLE

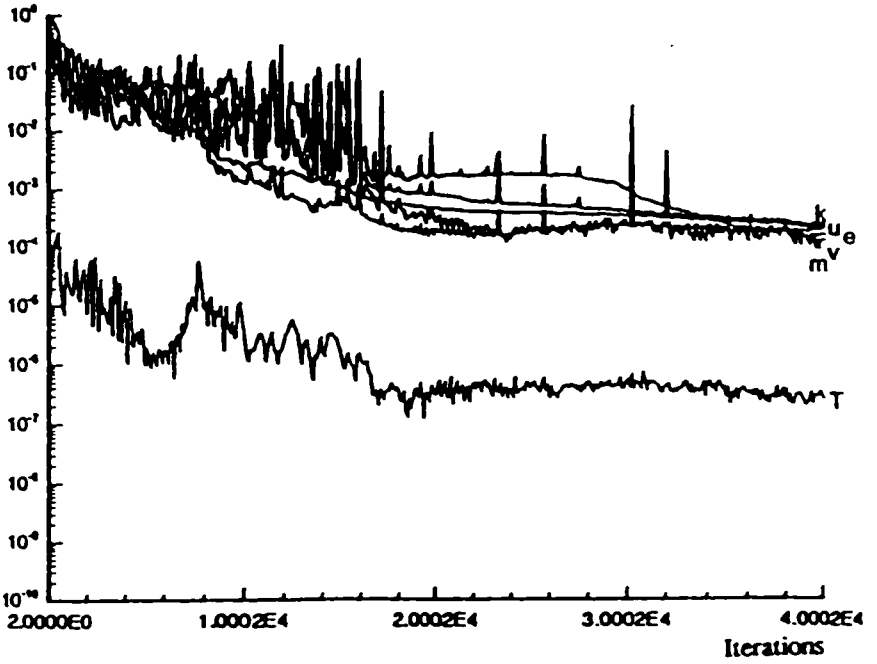

Fig. 23 (b) Residual Histories For Case B Using SIMPLET

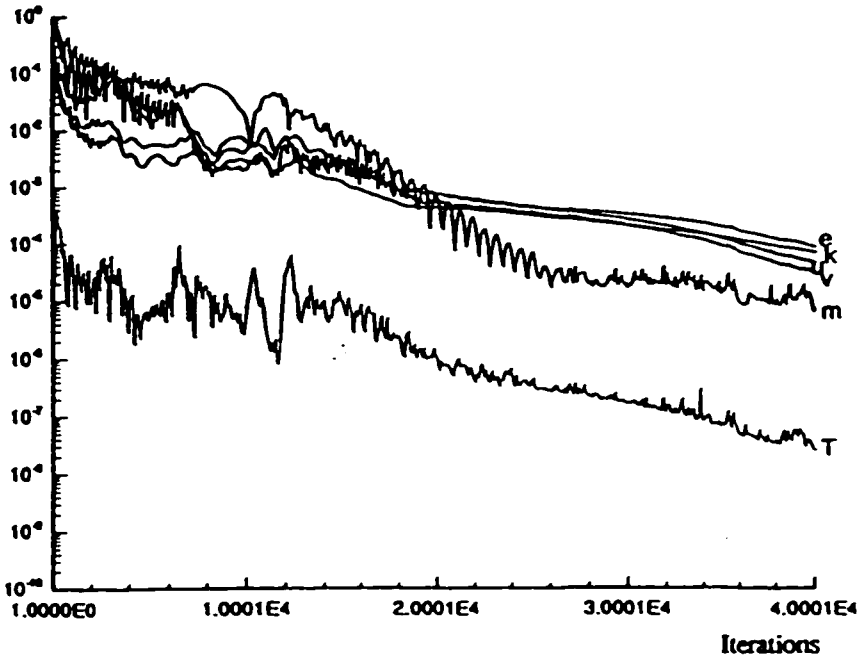

Fig. 24 (a) Residual Histories For Case C Using SIMPLE

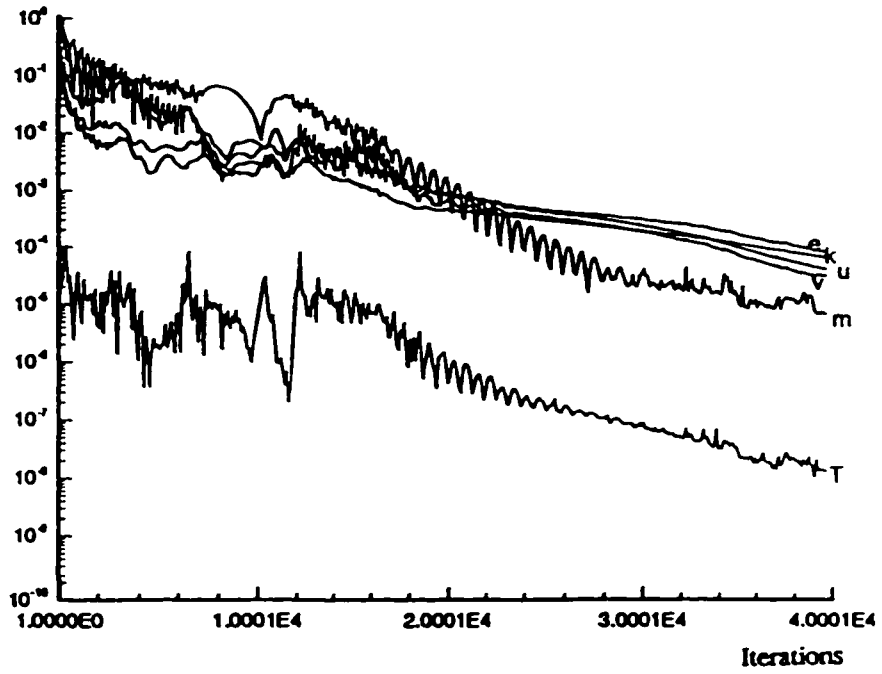

Fig. 24 (b) Residual Histories For Case C Using SIMPLET

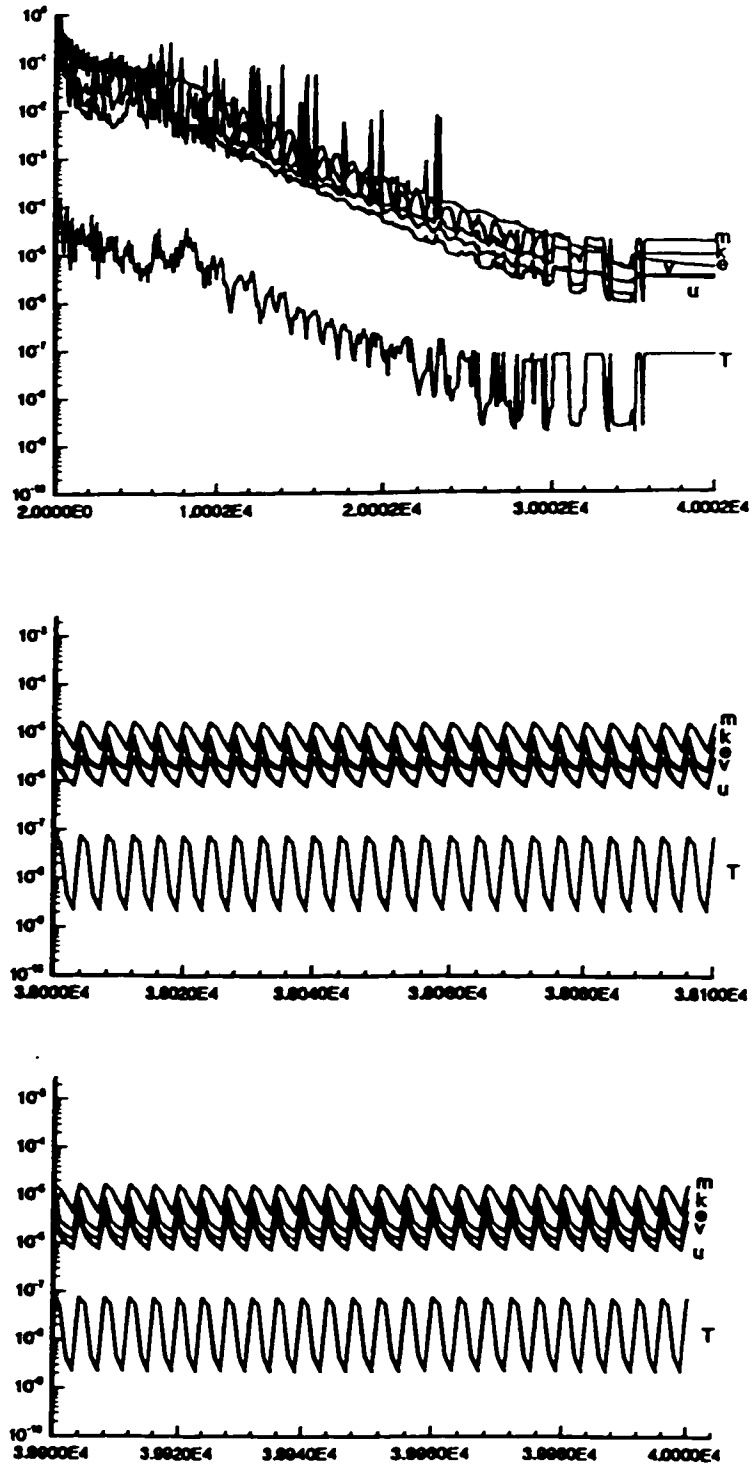

Fig. 25 (a) Residual Histories For Case A With Duct Width Equal To 12.7 mm Using SIMPLE

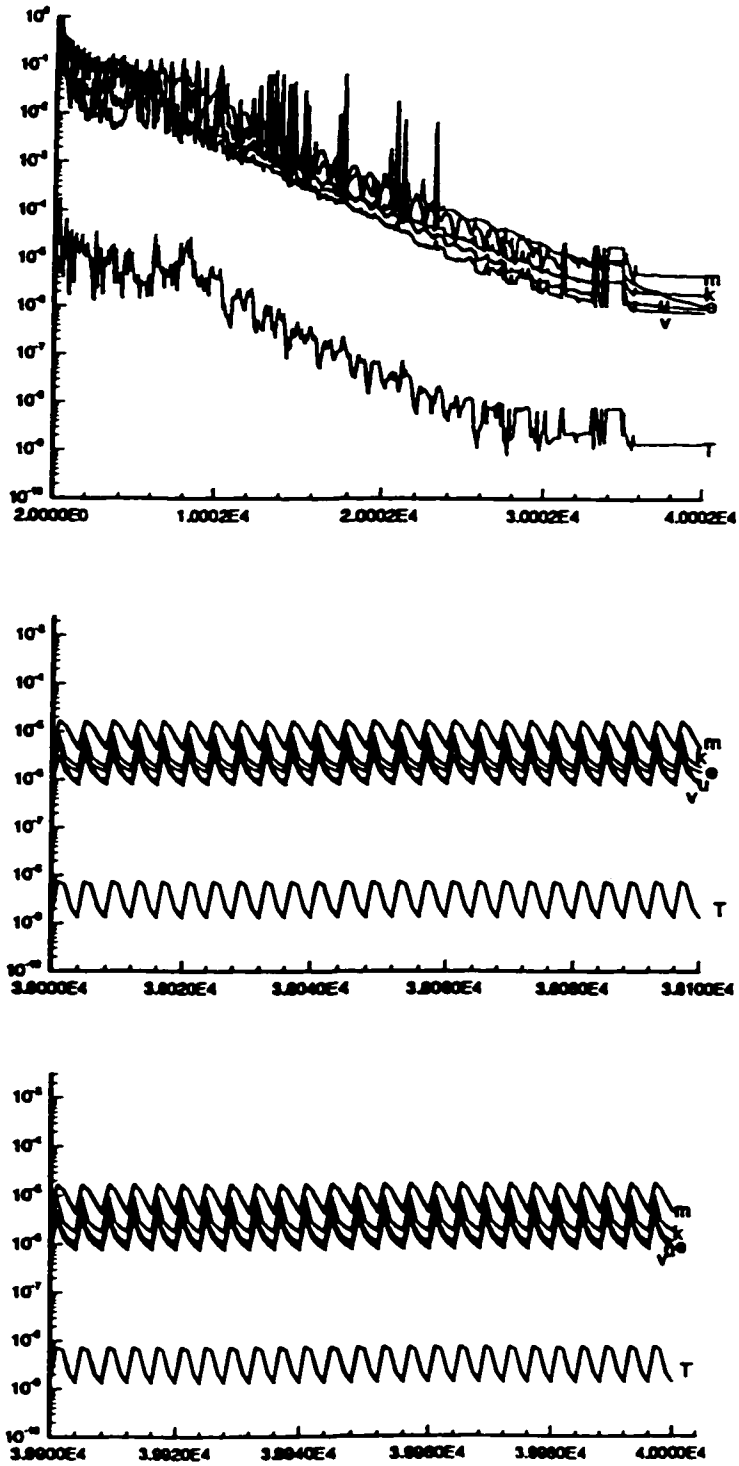

Fig. 25 (b) Residual Histories For Case A With Duct Width Equal To 12.7 mm Using SIMPLET

CHAPTER 6

DISCUSSION AND CONCLUSIONS

The major contribution of this thesis is the development of a new algorithm, SIMPLET, for solving buoyancy-driven flows. It can be applied to natural convection flows or mixed convection flows, laminar flows or turbulent flows.

The judgement of a converged solution used in this thesis is based on the commonly used convergence criteria recommended in FLUENT. The convergence criterion for temperature, T, is Res $\leq$ $1.0 \cdot 10^{-6}$ while the convergence criteria for the other variables are Res $\leq$ $1.0 \cdot 10^{-3}$. This work further proved that the smaller convergence criterion for temperature was necessary. In fact, even if this criterion is satisfied, in certain cases, the temperature has not yet reached convergence. Fig. 26 shows the test results for variable profiles at the outlet section F-F' after different iterations for test case A but with the duct width increased to 12.7 mm from 8.0 mm used in chapter 5. It can be seen that a more strict criterion for T is required in this case to ensure convergence. When precise predictions are required, more attention should be paid to the temperature convergence check.

The turbulence model used in the test cases is the RNG turbulence model with a two-layer model wall treatment. Because of the difficulties in modeling the turbulence

behavior in buoyancy-driven flows [41], the numerical results using the RNG model are still not totally satisfactory. However, this work does provide one more example to support the RNG turbulence model. For buoyancy driven flows such as the test case B in this thesis, the RNG turbulence model provides better results than proper low-Reynolds number k-ε turbulence models do (see Fig.21). In the RNG turbulence model, the low-Reynolds number effect is considered not only in the expression of μ_t, but also in the k and ε equations. The turbulent Prandtl numbers α_k, α_ε, α in the k, ε, T equations are no longer constants but are a function of μ_t/μ_l . The extra term in the ε equation captures the sensitivity of turbulence to streamline curvature and therefore makes the model suitable for a wide range of flows with serious separation and complex recirculation zones. The coefficient treatments in the RNG turbulence model can be considered to be quite universal for low Reynolds turbulent flows. The two layer zonal model successfully replaces the wall function treatment which is only applicable to simple and high Reynolds number turbulent flows.

The development of SIMPLET is divided into two stages. The author started this work from the CELS method developed by Galpin and Raithby [13]. The central concept of their method was to solve the continuity equation, the momentum equations and the energy equation simultaneously. The temperature velocity coupling in the momentum equations is created by introducing the Boussinesq approximation and is created by Newton-Raphson linearization in the energy equation: the nonlinear heat flux term, uT becomes

$$uT = u^*T + T^*u - u^*T^*$$

where the superscript * denotes the values from the previous iteration. The final equation set along a constant y grid line, the grid line j, is as follows[13]:

$$A^c_E u_i + A^c_W u_{i-1} + A^c_N v_i + b^c = 0$$

$$A^u_p u_i = A^u_E u_{i+1} + A^u_W u_{i-1} + A^{u,p}_p p_i + A^{u,p}_E p_{i+1} + A^{u,T}_p T_i + A^{u,T}_E T_{i+1} + b^u$$

$$A^v_p v_i = A^v_E v_{i+1} + A^v_W v_{i-1} + A^{v,p}_p p_i + A^{v,T}_p T_i + b^v$$

$$A^t_p T_i = A^T_E T_{i+1} + A^T_W T_{i-1} + A^{T,u}_E u_i + A^{T,u}_W u_{i-1} + A^{T,v}_N v_i + b^T$$

where the velocity components u, v , the pressure, p, and the temperature, T are the four variables to be solved. Their subscripts, i-1, i, i+1, denote the grid point location along the x direction. All the coefficients A and b with different superscripts and subscripts are constants. They are determined based on the currently available field values and the time step for unsteady flows or the under relaxation factor for steady flows. Since an efficient solver was developed to solve the equation set simultaneously, it usually provides faster convergence than the SIMPLE family of algorithms does when a converged solution can be reached. The detailed development and its performance shown in [13] encouraged the author to try its application to mixed convection flows. Though the possibility of its application to mixed convection flow can not be excluded, the difficulty is obvious. The simultaneous solution method was originally developed for solving linear coupled equations. Here, the equations are nonlinear and the iteration method is combined into the simultaneous solution procedure to linearize each of the individual equations. The coefficients and constants in the equations to be solved simultaneously must be updated after each iteration. Thus the method is only a partly simultaneous solution method and

the iteration procedure plays an important role in the solution procedure. When the equations are solved one by one using the sequential method, the under-relaxation factors introduced to prevent divergence in each equation can be different. In fact, the under relaxation factors for u and v equations are usually the same, but different for other equations. When the four equations are solved simultaneously, logically, the under relaxation factors should be kept the same. If different under relaxation factors for each equation are still used, one under relaxation factor will not only influence one equation but also influence the other equations since the equations are solved simultaneously. Therefore, the methodology of using the under relaxation factor to prevent divergence cannot be freely and effectively applied to the simultaneous solution method. It is not accidental that there is no application of the CELS method to mixed convection flows in the open literature. The latest open publication related to CELS method is still for natural convection flows [50].

Based on over half a year's work, the author decided to apply the velocity temperature coupling concept involved in the CELS method only and give up using the simultaneous solution procedure and returned back to using the SIMPLE family of algorithms. The idea of velocity temperature coupling also originated with the observation that the introduction of the Boussinesq approximation into the momentum equations made the solution easier to converge when the SIMPLE algorithm was used. By introducing the Boussinesq approximation, a direct link between the velocity and temperature was established, and the temperature, T, was treated as an explicit variable in the discrete momentum equations. These considerations prompted the author to make

the linkage of the velocity correction and the temperature correction in the pressure linked equation and in the whole solution procedure to speed up the convergence rate. Meanwhile, based on the physical analyses of buoyancy-driven flows, there are potentially two major forces which drive the fluid movement: the force caused by the temperature gradient and the force caused by the pressure (including kinetic pressure) gradient. From a logical point of view, the pressure linked equation should also be modified to include buoyancy effects. The SIMPLET method was then developed for buoyancy-driven flows. The derivation of the pressure linked equation considers the velocity changes to be caused by both pressure changes and temperature changes. For most laminar flows, where the velocity and temperature coupling is important, the SIMPLET method usually provides faster convergence than the traditional SIMPLE method. Like all the other algorithm modifications, the faster convergence benefit of SIMPLET is conditional, but it can be applied to both natural convection flows and mixed convection flows.

The second stage of the SIMPLET development started with the intention of applying the algorithm to the real industrial problems where the temperature variation in the flow field becomes significant and the Boussinesq assumption is not appropriate. Fortunately, the analysis of the SIMPLET algorithm development shows that we only need to link the velocity change and temperature change in the pressure linked equation and the solution procedure. It is not necessary to follow through with the mathematical treatment by introducing a volumetric thermal expansion coefficient to consider the effect of temperature change in the momentum equation and the pressure linked equation. A

new version of SIMPLET was then developed for the general cases of buoyancy-driven flows. Since large temperature variations invariably cause turbulence, the new version of SIMPLET was tested for turbulent flows. In retrospect, it was not necessary to have developed the old SIMPLET version first. The original intention of this thesis project was to extend the application of the CELS method, ie., to apply it to mixed convection flows. The SIMPLET development initially grew out of a study of the CELS method and adopted a key point of the CELS method: introducing the Boussinesq assumption to create the velocity temperature coupling. It was not until the initial SIMPLET method was developed, did the author realize that this restriction can be removed.

As mentioned in chapter 4, the faster convergence benefit using a particular algorithm is always conditional. When the pressure-velocity coupling is the factor mainly responsible for slow convergence, the SIMPLEC usually provides faster convergence than SIMPLE does [6]; Compared with the SIMPLE method, when the temperature-velocity coupling is the factor mainly responsible for slow convergence, the SIMPLET method usually provides faster convergence. However, in turbulent flows, the interaction between the turbulence model and the momentum equations is usually the factor mainly responsible for slow convergence. In such cases, the convergence rates of k, ε, u and v are the determinants in reaching a solution if the convergence criteria set in FLUENT [16] are used (ie. the normalized residual of temperature be less than $1.0 \cdot 10^{-6}$ and the normalized residuals of other variables less than $1.0 \cdot 10^{-3}$). Therefore, any SIMPLE family algorithm does not show dramatic advantages over the simplest scheme,

SIMPLE [49]. The SIMPLET method is not exceptional. Only in certain cases, such as test case B in chapter 5, where the driving forces are nearly in balance, does the convergence rate of T become the determinant in reaching a solution. Here SIMPLET will provide faster convergence. Fig. 27 shows a direct comparison of the energy equation convergence histories using SIMPLE and SIMPLET for test case B in chapter 5. While a converged solution is obtained using SIMPLET after 20000 iterations, the SIMPLE method never provides a converged solution if the convergence requirement of the normalized residuals on all the variables is strictly satisfied. I do not discount the possibility that a solution may be obtained with SIMPLE when more tests of underrelaxation factors are conducted. However, in all the cases tested, the SIMPLET method always provides a faster convergence rate for the energy equation than SIMPLE does. When the convergence rate of the energy equation becomes the determinant in reaching a solution, the advantage of the SIMPLET method will be prominent.

When the conventional SIMPLE family of methods is used to solve flows dominated by buoyancy with a weak pressure field, some special considerations must be taken to approach a converged solution. In the FLUENT software package, for example, several solution options are recommended for flows with strong body forces [16]. In his review paper in 1994 [41], Hanjalic mentioned that " most users employ the numerical solvers developed for pressure dominated forced flows, in which the pressure field is corrected in the course of numerical iteration to satisfy the continuity of the mean velocity field. This approach is inadequate for flows dominated by buoyancy with weak pressure field. An efficient solver with a better numerical coupling of the temperature

and velocity fields dominated by buoyancy is needed, particularly for more complex flows". The work done in this thesis strongly supports his argument. It does show that it is possible to find a way to couple the temperature and velocity using an iteration method for buoyancy-driven flows although the SIMPLET method is perhaps not the type of solver that Hanjalic has called for.

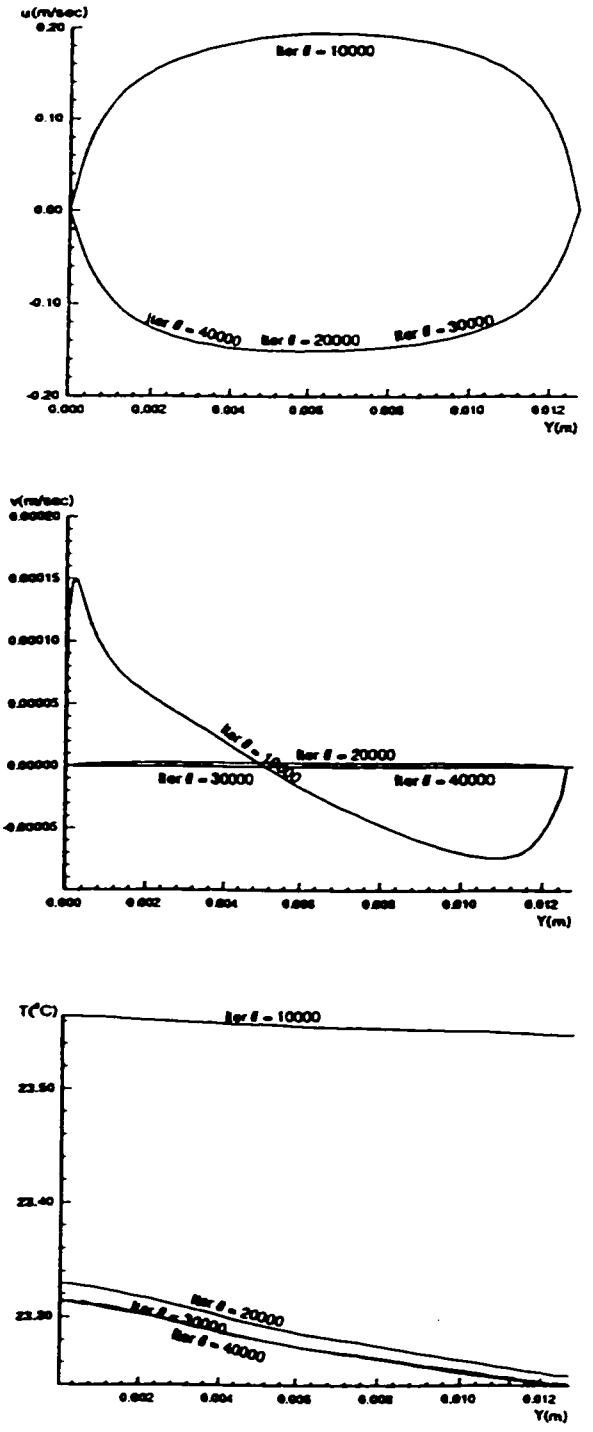

Fig. 26 Variable Profiles at the Outlet Section F'-F For Case A in Chapter 5

(Duct Width increased from 8 mm to 12.7 mm)

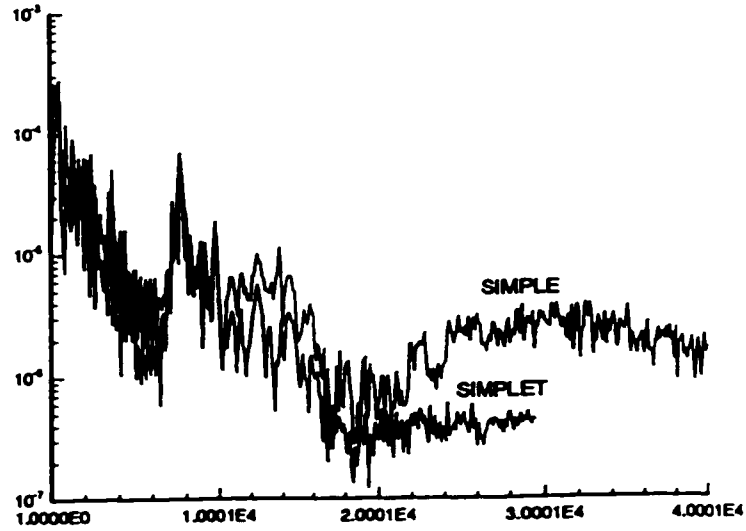

Fig. 27 Energy Equation Residual Histories For Test Case B

REFERENCES

1 Salik Kakac, and Yaman Yener, Convective Heat Transfer, CRC Press 1996.

2 C.A.J. Fletcher, Computational Techniques for Fluid Dynamics 1, Fundamental and General Techniques Springer-Verlag 1987.

3. J. H. Ferziger, M. Peric, Computational Method for Fluid Fynamics Springer, 1996.

4 S. V. Patankar, Numerical Heat Transfer and Fluid Flow, Hemisphere, Washington, D.C. 1980.

5 S. V. Patankar and D. B. Spalding, A Calculation Procedure for Heat Mass and Momentum Transfer in Three-Dimensional Parabolic Flows, International Journal of Heat and Mass Transfer, Vol. 15, PP 1787, 1972.

6 J. P. Van Doormaal, G. D. Raithby, Enhancements of the Simple Method for Predicting Incompressible Fluid Flows Numerical Heat Transfer Vol. 7, PP. 147-163, 1984.

7 R. I. Issa, Solution of the Implicitly Discretized Fluid Flow Equations by Operator-Splitting, Journal of Computational Physics 62, PP 40-65, 1985.

8 B. R. Latimer and A. Pollard, Comparison of Pressure-Velocity Coupling Solution Algorithms, Numerical Heat Transfer, Vol. 8, PP 635-652, 1985.

9 A. U. Chatwani and A. Turan, Improved Pressure-Velocity Coupling Algorithm Based on Minimization of Global Residual Norm, Numerical Heat Transfer, Part B,Vol.20, PP 115-123, 1991.

10 S. L. Lee and R. Y. Tzong, Artificial Pressure for Pressure-Linked Equation, International Journal of Heat and Mass Transfer, Vol. 35, No.10, PP 2705-2716, 1992.

11 R-H Yen and C-H Liu, Enhancement of the SIMPLE Algorithm by an Additional Explicit Corrector Step, Numerical Heat Transfer, Part B, Vol. 24, PP 127-141, 1993.

12 P. F. Galpin, Van. Doormaal, and G. D. Raithby, Solution of the Incompressible Mass and Momentum Equations by Application of a Coupled Equation Line Solver, Int. J. Numer. Methods Fluids, Vol. 9, PP 241-246, 1986.

13 P. F. Galpin and G. D. Raithby, Numerical Solution of Problems in Incompressible Fluid Flow: Treatment of the Temperature-Velocity Coupling, Numerical Heat Transfer, Vol. 10, PP. 105-129, 1986.

14 L. Davidson, Calculation of the Turbulent Buoyancy-Driven Flow in a Rectangular Cavity Using an Efficient Solver and Two Different Low Reynolds Number k-ε Turbulence Models, Numerical Heat Transfer, Part A, Vol. 18, PP. 129-147, 1990.

15 Boussinesq, Theorie Analytique de la Chaleur, Vol 2. Gauthier-Villars, Paris, 1903

16 FLUENT Inc., FLUENT User's Guide Version 4.3, Jan. 1996.

17 G. De Vahl Davis, and I. P. Jones Natural Convection in a Square Cavity: A Bench Mark Numerical Solution, Int. J. Numerical Methods Fluids, Vol. 3, pp. 227-248, 1983.

18 H. I. Abu-Mulaweh, B.F. Armaly and T. S. Chen, Measurements in Buoyancy-Assisting Laminar Boundary Layer Flow Over a Vertical Backward-Facing Step—Uniform Wall Heat Flux Case, Experimental Thermal and Fluid Science 1993, 7, PP.39-48.

19 D. D. Gray and A. Giorgini, The Validity of the Boussinesq Approximation for Liquids and Gases, International Journal of Heat and Mass Transfer, vol. 19, pp. 545-550, 1976.

20 G. Numberg, P. Wood and M. Shoukri, Experimental and Numerical Turbulent Buoyancy Flow in an Enclosure, 10th Int. Heat Transfer Conf., PP 119-124, 1994.

21 J. Boussinesq Theorie de l'ecoulement Tourbillant, Mem. Pre. Par. Div. Sav. 23, Paris, 1877.

22 H. Tennekes and J. L. Lumley, A First Course in Turbulence, The MIT Press 1972.

23 B. E. Launder and D. B. Spalding, Lectures in Mathematical Modeling of Turbulence, Acadamic Press, 1972.

24 R. A. W. M. Henkes and C. J. Hoogendoorn, Comparision of Turbulence Model for the Natural Convection Boundary Layer Along a Heated Vertical Plate, Int. J. Heat Mass Transfer, Vol. 32, No. 1, pp. 157-169, 1989.

25 C. K. G. Lam and K. Bremhorst, A Modified Form of the k-ε Model for Predicting Wall Turbulence. J. Fluids Engng 103, pp. 456-460, 1981.

26 S. Hassid and M. Poreh, A Turbulent Energy Dissipation Model for Flows With Drag Reduction, J. Fluids Eng. 100, pp. 107-112, 1978.

27 G. H. Hoffman, Improved Form of the Low Reynolds Number k-ε Turbulence Model, Physics Fluids 18, pp. 309-312, 1975.

28 B. E. Launder and B. R. Sharma, Application of the Energy-Dissipation Model of Turbulence to the Calculation of Flow near a Spinning Disc. Lett. Heat Mass Transfer 1, pp. 131-138, 1974.

29 D. Dutoya and P. Michard, A Program for Calculating Boundary Layers Along Compressor and Turbine Blades. Numerical Methods in Heat Transfer. Wiley, New York, 1981.

30 K. Y. Chien, Predictions of Channel and Boundary-Layer Flows With a Low Reynolds Number Turbulence Model, AIAA J. 20, pp. 33-38, 1982.

31 W. C. Reynolds, Computation of Turbulent Flows, Ann. Rew. Fluid Mech. 8, pp. 183-208, 1978.

32 Y. Nagano and M. Hishida, Improved Form of the k-ε Model for Wall Turbulent Shear Flows, J. Fluids Engng 109, pp. 156-160, 1987.

33 J. Herrero, F. X. Grau, J. Grifoll and F. Giralt, A Near Wall k-ε Formulation for High Prandtl Number Heat Transfer, Int. J. Heat Mass Transfer. Vol. 34, No. 3, pp. 711-721, 1991.

34 W. M. To and J. A. C. Humphrey, Numerical Simulation of Buoyant, Turbulent Flow ---- I. Free Convection Along a Heated, Vertical, Flat Plate, Int. J. Heat Mass Transfer, Vol. 29, No. 4, pp. 573-592, 1986.

35 Lars Davidsion, Calculation of the Turbulent Buoyancy-Driven Flow in a Rectangular Cavity Using an Efficient Solver and Two Different Low Reynolds Number k - Turbulence Models, Numerical Heat Transfer, Part A, Vol. 18, pp. 129-147, 1990.

36 M. A. Cotton and J. D. Jackson, Vertical Tube Air Flows in the Turbulent Mixed Convection Regime Calculated Ussing a Low-Reynolds Number k-ε Model, Int. J. Heat Mass Transfer, Vol. 33, No. 2, pp. 275-286, 1990.

37 R. A. W. M. Henkes and C. J. Hoogendoorn, Natural Convection Flow in a Square Cavity Calculated with Low-Reynolds Number Turbulence Models, Int. J. Heat Mass Transfer, Vol. 34, No. 2, pp. 377-388, 1991.

38 B. J. Daly and F. H. Harlow, Transport Equations in Turbulence, Physics Fluids 13, PP.2634-2649, 1970.

39 N. Z. Ince and B. E. Launder, On the Computation of Buoyancy-driven Turbulent Flows in Rectangular Enclosures, Int. J. Heat and Fluid Flow. Vol. 10, No. 2, pp. 110-117, June 1989.

40 Lars Davidson, Secondorder Corrections of the k-ε Model to Account for Non-isotropic Effects due to Buoyancy, Int. J. Heat Mass Transfer, Vol. 33, No. 12, pp. 2599-2608, 1990.

41 R. Hanjalic, Achivements and Limitations in Modeling and Computation of Buoyancy Turbulent Flows and Heat Transfer, Heat Transfer, Institution of Chemical Engineers Symposium Series Vol. 135/1 1994.

42 W. K. George and S. P. Capp A Theory for Natural Convection Turbulent Boundary Layers Next to Heated Vertical Surfaces, Int. J. Heat Mass Transfer, Vol. 22, PP. 813-826

43 V. Yakhot and S. A. Orszag, Renormalization Group Analysis of Turbulence, Journal of Scientific Computing, Vol. 1, No. 1, 1986.

44 B. E. Launder, On the Computation of Convective Heat Transfer in Complex Turbulent Flows, Journal of Heat Transfer, Vol. 110, pp. 1112-1128, Nov.1988.

45 Y. G. Lai and R. M. C. So, Near-wall Modelling of Turbulent Heat Fluxes, Int. J. Heat Mass Transfer, Vol. 33, No. 7, pp.1429-1440, 1990.

46 Lars Davidson, Secondorder Corrections of the k-ε Model to Account for Non-isotropic Effects due to Buoyancy, Int. J. Heat Mass Transfer, Vol. 33, No. 12, pp. 2599-2608, 1990.

47 Z. U. A. Warsi, Fluid Dynamics, Theoritical and Computational Approaches, CRC Press, 1993.

48 S. Ostrach, Natural Convection in Closures, J. Heat Transfer, Vol. 110, PP. 1175-1190, 1988.

49 M. A. Leschziner, Modeling Turbulent Recirculating Flows by Finite-volume Methods ----Current Status and Future Directions, Int. J. Heat and Fluid Flow, Vol. 10, No. 3, pp. 186-202, Sept. 1989.

50 G. B. Deng, J. Piquet, P. Queutey, M. Visonneau, Incompressible Flow Calculations with a Consistent Physical Interpolation Finite Volume Approach, Computers Fluids, 23, PP. 1029-1047, 1994.